AFFINITY OF GLYCOPEPTIDE NANOFIBERS TO GROWTH FACTORS AND THEIR EFFECTS ON CELLS

A THESIS SUBMITTED TO

THE GRADUATE SCHOOL OF ENGINEERING AND SCIENCE

OF BILKENT UNIVERSITY

IN PARTIAL FULFILLMENT OF THE REQUIREMENTS FOR

THE DEGREE OF

MASTER OF SCIENCE

IN

MATERIALS SCIENCE AND NANOTECHNOLOGY

By

NURCAN HAŞTAR

September, 2017

AFFINITY OF GLYCOPEPTIDE NANOFIBERS TO GROWTH FACTORS

AND THEIR EFFECTS ON CELLS

By Nurcan Haştar,

September, 2017

We certify that we have read this thesis and that in our opinion it is fully adequate, in scope and in quality, as a thesis for the degree of Master of Science.

_____

Michelle Marie Adams (Advisor)

_____

Ayşe Begüm Tekinay (Co-Advisor)

_____

Çağlar Elbüken

_____

Melih Önder Babaoğlu

Approved for the Graduate School of Engineering and Science:

_____

Ezhan Karaşan

Director of the Graduate School of Engineering and Science

ABSTRACT

AFFINITY OF GLYCOPEPTIDE NANOFIBERS TO GROWTH FACTORS AND THEIR EFFECTS ON CELLS

Nurcan HAŞTAR

M.Sc. in Material Science and Nanotechnology

Advisor: Michelle Marie Adams

Co-Advisor: Ayşe Begüm Tekinay

September, 2017

The development of scaffolds for growth factor delivery is a promising approach for tissue regeneration applications due to their crucial roles during regeneration. Growth factor secretion and interactions with glycosaminoglycans are essential steps for the regulation of cellular behavior. Therefore, glycosaminoglycan-mimetic scaffolds provide a great opportunity to modulate the effects of growth factor actions on cell fate. In this thesis, sugar-bearing peptide amphiphile molecules were characterized and tested for VEGF, FGF-2 and NGF affinity. ELISA-based affinity analyses revealed that glycopeptide nanofibers had high affinity to NGF; however, glycopeptides alone were not enough to interact efficiently with VEGF and FGF-2. Since VEGF and NGF contain heparin-binding domains, the addition of a sulfonated peptide amphiphile increased the affinity of the nanofiber network to these growth factors. Glycopeptide-sulfonate nanofibers were also found to promote *in vitro* tube formation through their VEGF and FGF-2 affinity. VEGF release profiles of HUVECs indicated that increasing concentration of VEGF may provide autocrine signaling and enhance tube

formation without any exogenous pro-angiogenic factor addition. In addition, when NGF-responsive PC-12 cells were cultured on glycopeptide nanofibers, they extended their neurites to an extent comparable with a widely-used positive control molecule (poly-L-lysine). These results suggest that glycosaminoglycan-mimetic glycopeptide nanofiber networks can be used as efficient growth factor presentation platforms for tissue regeneration applications to induce angiogenesis or peripheral nerve regeneration.

KEYWORDS: Growth factors, glycosaminoglycans, extracellular matrix, peptide nanofibers, neovascularization, neurite extension

ÖZET

BÜYÜME FAKTÖRLERİNİN ŞEKERLİ NANOFİBERLERE AFİNİTESİ VE BU NANOFİBERLERİN HÜCRELERE ETKİLERİ

Nurcan HAŞTAR

Malzeme Bilimi ve Nanoteknoloji, Yüksek Lisans

Tez Danışmanı: Michelle Marie Adams

Tez Eşdanışmanı: Ayşe Begüm Tekinay

Eylül, 2017

Büyüme faktörleri, doku yenilenmesi sırasında önemli görevler almaktadırlar. Bu nedenle büyüme faktölerinin etkili bir biçimde hedeflenen bölgeye ulaştırılması doku yenilenmesi çalışmaları için önem taşımaktadır. Büyüme faktörlerinin glikozaminoglikanlarla etkileşimleri, fonksiyonlarını doğru bir şekilde yerine getirmeleri için önemli bir basamaktır. Bu sebeple, glikozaminoglikan benzeri yapıların büyüme faktörlerinin sunulması için tasarlanan yapı iskelelerinde kullanımları doku yenilenmesi için umut vaat eden bir yaklaşımdır. Bu çalışmada, glikozaminoglikanların monomerlerine benzer şekerli peptit nanofiberlerin, vasküler endotelyal büyüme faktörü (VEGF), fibroblast büyüme faktörü (FGF-2) ve sinir büyüme faktörüne (NGF) olan afinitesi ve bu peptit nanofiberlerin hücrelere olan etkileri araştırılmıştır. Şeker içeren nanofiberler NGF'e kuvvetle bağlanma gösterirken, VEGF ve FGF-2 moleküllerine afinitelerinin daha az olduğu

gözlemlenmiştir. VEGF ve FGF-2, heparin bağlanma domaini içerdiği ve heparinde yüksek miktarda sülfat molekülü bulunduğu için, bu nanofiberlerin yapısına sülfatlı peptit amfifil molekülünün eklenmesi, bu büyüme faktörlerine olan afinitesini artırmıştır. Büyüme faktörlerinin şekerli nanofiberlere afiniteleri göz önüne alınarak, bu nanofiberlerin endotel ve NGF'e yanıt veren PC-12 hücrelerine olan etkileri incelenmiştir. Sonucunda endotel hücreleri ekstra büyüme faktörüne ihtiyaç duymadan tüp benzeri yapılar oluşturmuş ve PC-12 hücreleri yüksek oranda nörit uzatmışlardır. Bu sonuçlar değerlendirildiğinde, üretilen şekerli yapı iskeleleri, yeni damar oluşumu gereken durumlarda ve periferik sinir yaralanmalarının onarımında, büyüme faktörlerinin etkili sunulması için *in vivo* çalışmalarda uygun birer platform sağlayabilirler.

ANAHTAR SÖZCÜKLER: Büyüme faktörleri, glikozaminoglikanlar, ekstraselüler matriks, peptit nanofiberler, yeni damar oluşumu, nörit uzatımı

ACKNOWLEDGEMENTS

Contents

LIST OF FIGURES

x

Abbreviations

AFM	Atomic force microscopy
ANOVA	Analysis of variance
CD	Circular dichroism
DCM	Dichloromethane
DIEA	*N,N*-diisopropylethylamine
DMEM	Dulbecco's modified Eagle's medium
DMF	N, N-Dimethylformamide
ELISA	Enzyme-linked immunosorbent assay
ECM	Extracellular matrix
FGF-2	Fibroblast growth factor-2
FBS	Fetal bovine serum
Fmoc	9-Fluorenylmethoxycarbonyl
GAG	Glycosaminoglycan
GF	Growth Factor
HBTU	*N,N,N′,N′*-Tetramethyl-O-(1*H*-benzotriazole-1-yl) uronium hexafluorophosphate
HUVEC	Human umbilical vein endothelial cell
LC-MS	Liquid chromatography-mass spectroscopy
NGF	Nerve growth factor
PA	Peptide amphiphile
SEM	Scanning electron microscopy
TCP	Tissue culture plate
TFA	Trifluoroacetic acid
TIS	Triisopropyl silane

Chapter 1

1. Introduction

1.1. Carbohydrates of Extracellular Matrix

All cells of the human body are surrounded by an extracellular matrix (ECM) that contributes to their behaviors despite not strictly being a part of the cell environment. Components of ECM demonstrate tremendous variety but mainly consist of proteins, carbohydrates, and complexes formed by the combination of both (Figure 1). Biomechanical characteristics of ECM, as well as the composition and spatiotemporal orientations of its components, may differ depending on tissue type. In addition to providing mechanical support to cells, this network delivers signals to regulate cellular activities such as migration, differentiation, and proliferation through its dynamic properties [4].
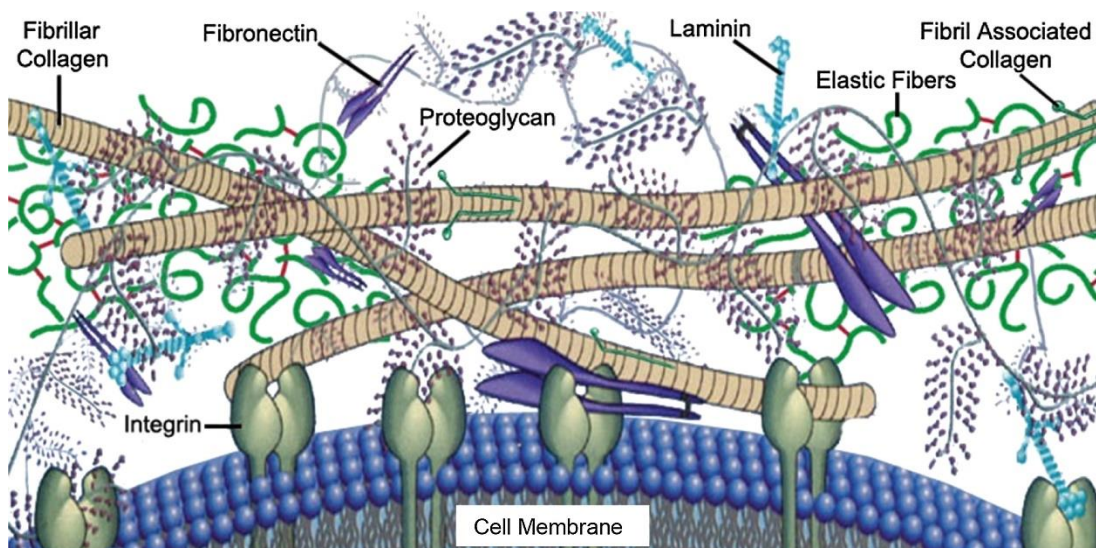
Figure 1: Representative image of the extracellular matrix. Structural proteins such as collagen provide physical support. Adhesive proteins like laminin and fibronectin function by interacting with integrin. Carbohydrate components of ECM, proteoglycans and connected unbranched glycosaminoglycans, have distinct biological functions. Copyrighted from © 2016 Elsevier Ltd. Published by Elsevier.

Two main types of ECM elements are glycosaminoglycans, which are typically bound to protein cores and called proteoglycans in this form, and fibrous proteins such as collagen, elastin, laminin, and fibronectin that are responsible for structural support by forming the fibrillary structures of the ECM and assisting in cell adhesion [5-6]. Collagens are the most abundant proteins of ECM, and twenty-eight different types of collagen have so far been defined in the literature [5]. These tensile fibers resist deformation during the mechanical stretching of tissues [7]. Collagen deposition is performed by tissue-specific cells in connective tissues, *e.g.* collagens are secreted from osteoblasts in bone and from chondroblasts in cartilage tissue. In addition, a small percentage of collagen molecules are modified with monosaccharides and disaccharides [8]. In contrast to collagen, elastin mediates stretching in response to mechanical forces and provides elasticity to tissues like elastic cartilage, arterial vessels, and lungs. Elastins form microfibril-coated fibers that contain glycoproteins called fibrillins, which are members of the fibronectin family and are crucial for elastin function. Due to their strongly hydrophobic amino acid composition, elastins are able to recover their original shapes after exposure to mechanical forces [9]. While collagens and elastins provide physical support and are the main structural components of the ECM, glycoproteins are responsible for mediating cellular adhesion. Fibronectin is one of the glycoproteins of the ECM and assists in the adhesion of cells to their ECM [10] or facilitates their migration at some of the crucial events during development [11]. It has several domains that interact with other ECM structures such as heparin, proteoglycans, glycosaminoglycans, and fibrin, as well as transmembrane receptors called integrins [12]. Epithelial cells and fibroblasts are the main cell types that secrete

fibronectin. In the ECM, secreted fibronectins form fibrils and can be found in the solid state, while the soluble form of fibrils are found in body fluids such as blood [13]. Laminin is mainly synthesized by neurons, bone marrow cells, muscle cells and the epithelium, and it is a main component of the basal lamina [6]. This glycoprotein is formed by three different elongated polypeptides and has various domains that are recognized by some of the glycosaminoglycans, integrins and type IV collagen. It mediates the interaction between basement membrane, type IV collagen and cells, and establishes a connection between cell adhesion sites and the ECM network [14].

Glycosaminoglycan (GAG) units of proteoglycans are the carbohydrate reservoir of the ECM. Proteoglycans can be thought of as a storage unit containing GAGs that are covalently attached to a core protein. Proteoglycans can be found in intracellular sites, cell membranes, and the ECM environment. Their interactions with ECM molecules, growth factors, chemokines or receptors are mediated by their core proteins or attached GAG sites. These interactions result in the organization of the ECM and behaviors such as adhesion, proliferation, differentiation or migration [15]. Unbranched polysaccharides that either reside freely in the ECM or connect to proteoglycans through one or more binding sites are called glycosaminoglycans. GAGs are composed of disaccharide units. One saccharide unit is an amino sugar (D-galactosamine or D-glucosamine) and the second unit is uronic acid (D-glucuronic acid or L-iduronic acid) [16]. Anionic characteristics of GAGs arise from the presence of carboxyl and sulfate groups on some of the sugar subunits. Due to negatively-charged subunits, GAGs have the capacity to absorb high amounts of water and form a gel-like environment for cells. These hydrated gels help to absorb mechanical forces and provide transportation of molecules from the ECM to cells. Their sugar subunits can be sulfated at carbon 4 or

6 or non-acetylated nitrogen atoms, increasing the diversity of GAG chains. This sulfation arrangement leads to the formation of over 1,000,000 different patterns [17].

Glycosaminoglycan	Disaccharide units	Uronic acid	Hexosamine
Hyaluronic acid (HA)	D-GlcA-β(1→4)-D-GlcNAc-α(1→4)	Glucuronic	Glucosamine
Chondroitin sulfate (CS)	D-GlcA-β(1→3)-D-GalNAc4S-β(1→4)	Glucuronic	Galactosamine
Dermatan sulfate (DS)	L-IdoA-α(1→3)-D-GalNAc4S-β(1→4)	Iduronic	Galactosamine
Keratan sulfates I and II (KS)	D-Gal-β(1→4)-D-GlcNAc6S-β(1→3)	Glucuronic	Glucosamine
Heparin (HP)	L-IdoA2S-α(1→4)-D-GlcNAc6Sα(1→4)	Iduronic	Glucosamine
Heparan sulfate (HS)	D-GlcA-β(1→4)-D-GlcNAcα-(1→4)	Glucuronic	Glucosamine
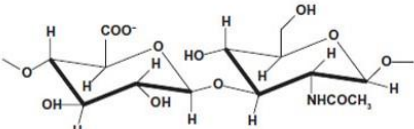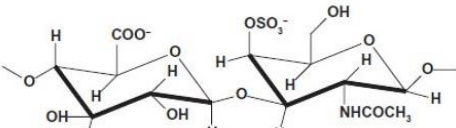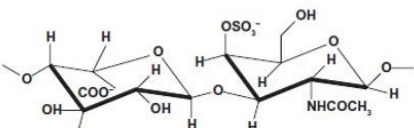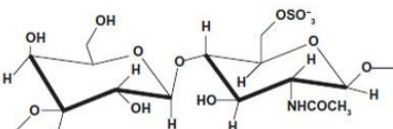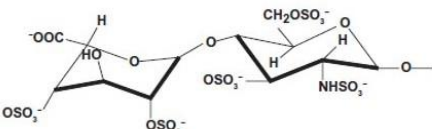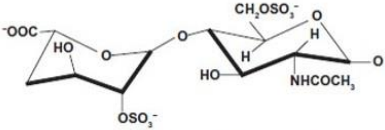
Figure 2: Chemical structures of glycosaminoglycans. Disaccharide units and their linkage types are provided with their common names. Copyright© 2013, Dovepress [2].

Six types of GAGs are present in ECM and are classified depending on the type of their saccharide unit and its glycosidic linkage (Figure 2). Only one type does not contain sulfated saccharide units and is called hyaluronic acid (HA, hyaluronate, hyaluronan). Hyaluronic acid is composed of D-glucuronate (GlcA) and N-acetylglucosamine (GlcNAc), which is linked through β (1, 3) glycosidic bonds. HA is non-epimerized and does not have any connection with core proteins of the ECM. It is mostly found in the synovial fluid, articular cartilage, vitreous humor, skin and loose connective tissue [18]. Other types of GAGs are chondroitin sulfate (CS), dermatan sulfate (DS), keratan sulfate (KS), heparin (HP) and heparan sulfate (HS). CS is the most abundant GAG and consists of GlcA and GalNAc-4 or 6 sulfate with a β (1, 3) linkage. CS is attached to core proteins of proteoglycans called lecticans. Versican, aggrecan, and decorin are members of this family. CS participates in developmental stages of the central nervous system, the wound healing process and various signaling events resulting in cell division and morphogenesis. It is a major component of the tendons, aorta, cornea, bone, cartilage and intervertebral discs [19]. DS is related to CS and was previously classified as chondroitin sulfate B. The amino sugar component of DS is N-acetylgalactosamine (GalNAc), which is sulfated at position 4 and are linked by a β (1,3) bond to GlcA or an α (1,3) bond to L-iduronate (IdoA). It is found in skin, lung, heart valves and blood vessels and plays a role in clot formation, wound healing, fibrous tissue production and infection [20]. Disaccharide units of keratan sulfate consist of β (1,4) linked galactose and GlcNAc, which is sulfated at the sixth carbon. This GAG appears in the brain, cornea and cartilage tissues, and binds to

keratocan, lumican, and aggrecan proteoglycans to assist in the cell movement, axon guidance and ligand recognition [21]. Heparin (HP) and heparan sulfates share identical disaccharide units, which are IdoA (typically sulfated at the 2 position) or GlcA (also typically sulfated at the 2 position) linked to N-sulfo-D-glucosamine-6-sulfate with α (1,4) (if IdoA) or β (1,4) (if GlcA) bonds, but heparin has a much higher sulfate content than heparan sulfate. Due to its highly negative charge, HP forms strong electrostatic interactions with thrombin and serves as an anticoagulative agent. Mast cells store heparin in their intracellular compartments, and the GAG is also present in the arteries of the lungs, liver, and skin [22]. Heparan sulfate is a fundamental type of GAG for the ECM and basement membranes of cells. HS contains more acetylated glucosamine and interacts with syndecans and glycosylphosphatidylinositol (GPI)-linked glypicans. In addition, it has an affinity to growth factors such as fibroblast growth factor (FGF), vascular endothelial growth factor (VEGF), hepatocyte growth factor (HGF) and chemokines [23].

1.2. Growth Factors and Their Interaction with Glycosaminoglycans

A wide range of growth factors is required to orchestrate and regulate the physiological functions of tissues. Growth factors are secreted polypeptides that participate in crucial steps of development, regeneration, and morphogenesis. They exert their effects by interacting with specific receptors on the cell membrane. Receptor-growth factor interactions result in the activation of associated pathways by phosphorylating the internal domain of receptors. Pathway activation regulates the expression or inhibition of related genes, which typically modulate the survival, proliferation, differentiation or migration of cells (Figure 3) [3] [24].

Oxygen is an indispensable requirement of cells. Transportation of oxygen to cells and tissues is crucial for survival and facilitated by blood vessels. Therefore, the formation of new blood vessels from pre-existing ones (angiogenesis) is an essential event for wound healing and the regeneration of tissues. In addition, angiogenesis is observed in pathological processes such as metastasis and rheumatoid arthritis.
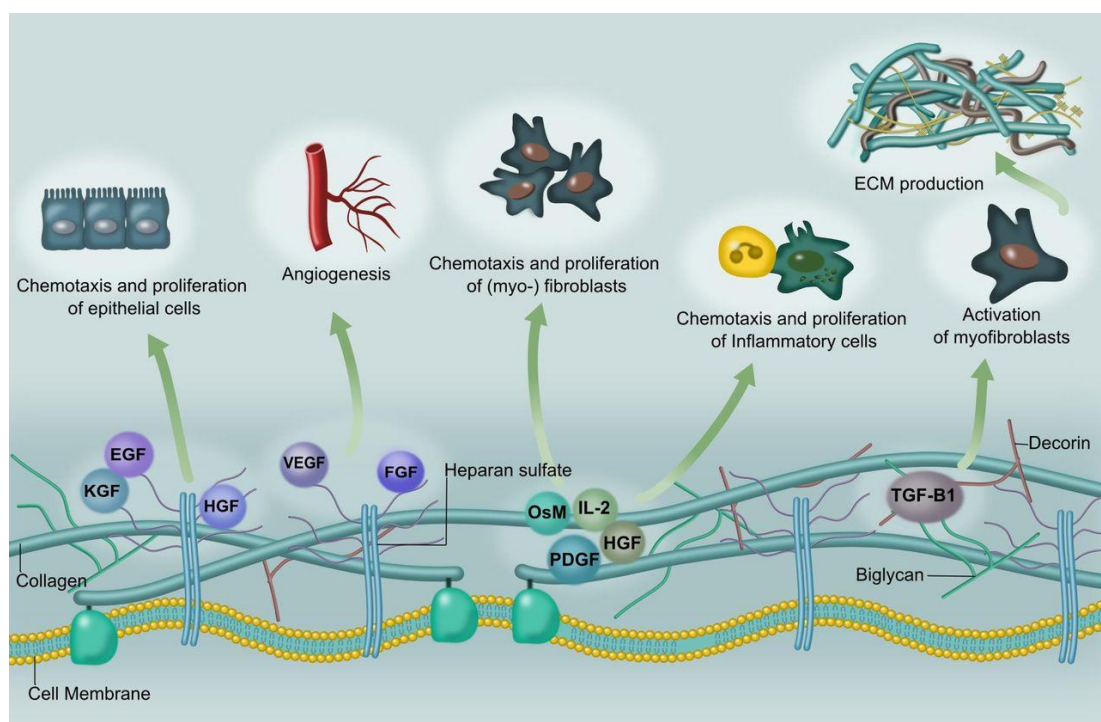
Figure 3: Growth factors bearing heparin-binding domains associate with heparan sulfate glycosaminoglycans and exert their effects depending on their type, which could be to mediate the differentiation, migration, proliferation processes of cells. Copyrighted from American Journal of Physiology - Gastrointestinal and Liver Physiology Published 15 May 2015 Vol. 308 no. 10, G807-G830 DOI: 10.1152/ajpgi.00447.2014 [3].

Endothelial cells undergo a differentiation during new blood vessel formation. After their division, some regions of the basement membrane and extracellular matrix near endothelial cells are partially degraded to allow their migration, which culminates in the formation of tubular structures [25]. Proangiogenic and antiangiogenic factors stay in balance under normal physiological conditions, resulting in the steady renewal of blood vessels. Vascular endothelial growth factor (VEGF) is one of the major proangiogenic signals. Interaction of VEGF with its receptor triggers a signaling pathway that results in the survival, growth, and migration of endothelial cells. Seven different types of VEGF have been described in the literature, called VEGF-A through VEGF-F, and placental growth factor (PlGF). Among them, VEGF-A is the major factor that is responsible for neovascularization. Alternative splicing of the VEGF-A transcript leads to seven isoforms that consist of distinct amino acid numbers; 121, 145, 148, 165, 183, 189, or 206 [26]. $VEGF_{165}$ is the most predominant form of VEGF-A and includes a C-terminal heparin binding domain. It can either be found free or bound to the ECM. In the ECM, VEGF interacts with the heparan sulfate (HS) GAG and/or heparin and neuropilin co-receptors through its heparin binding domain. In addition, HS and heparin interact with the VEGF receptor and mediate the stabilization of VEGF, neuropilin and its associated receptor complex. This complex increases the stability and lifetime of VEGF and provides controlled release and effective presentation of the growth factor by enhancing its affinity to its receptor. 6-O sulfation of the HS chain was previously indicated as an essential motif for the affinity of VEGF to HS [27].

Fibroblast growth factors have been identified at the beginning of the seventies and investigated extensively since then. Acidic and basic FGF were first described

according to their contribution to fibroblast growth and isoelectric points [28]. Following research characterized 20 sub-types of FGF. Although the name of FGF implies that its only function is related to fibroblast growth, FGF pathway actually regulates the development of embryonic tissues, maintains the homeostasis of tissues, and enhances regeneration and angiogenesis [29]. Acidic fibroblast growth factor (aFGF, FGF-1) and basic fibroblast growth factor (bFGF, FGF-2) are not by themselves sufficient to activate. Therefore, secreted FGF-1 and FGF-2 are bound to heparin sulfate proteoglycan (HSPG) and internalized directly into cells [30]. HS and HP can then interact with FGF and its receptor (FGFR) and stabilize this ternary complex by enhancing their interaction. HS triggers the dimerization of FGF and directs its interaction with the extracellular domain of FGFR. FGF binding leads to the dimerization of FGFRs, tyrosine kinase domains of which phosphorylate each other to start a signaling cascade [31]. FGF-HS interactions and ternary complex formation are regulated by the length and total charge density of sulfates, regardless of HS sulfation pattern [32]. As such, proper signaling of FGF requires HS since HS acts as a reservoir of FGF, protects it from degradation, and regulates its diffusion area.

Nerve growth factor (NGF) is one of the neurotrophic factors that are responsible for the proliferation, growth, and survival of the neurons of the peripheral nervous system. Expression of the NGF gene produces three proteins, which are alpha-, beta- and gamma-NGF. The functional form of NGF is formed when gamma subunit acts as a serine protease and separates the N-terminal of the beta subunit [33]. NGF has two known receptors; TrkA and p75^{NTR}. TrkA is the principal receptor and mediates fundamental responses of cells by interacting with NGF. Since TrkA is a kind of tyrosine kinase receptor, its interaction with NGF triggers its dimerization and

phosphorylation, which results in the activation of differentiation pathways [34]. Some neurotrophins, including NGF, exhibit affinity to the 4- and 6-O sulfated GalNAc epitopes of chondroitin sulfate. It has been shown that NGF association with CS leads to the assembly of a signaling complex and modulates related pathways [35]. However, exogenous presentation of CS to the culture medium of cells prevents the activation of NGF-TrkA by sequestering NGF and keeping it away from the cell membrane [36].

GAGs and proteoglycans are able to modulate the growth factor activity in the following ways: They can sequester growth factors to act as a natural reservoir of signaling molecules while delaying their immediate activity; they can preserve growth factors from proteolytic degradation and therefore extend their action time, and they can bring them to spatiotemporally appropriate positions to efficiently present them to cell surface receptors [32].

1.3. Growth Factor Presentation Strategies

Tissue engineering applications are improving day by day through an enhanced understanding of the biological, chemical and physical requirements of damaged tissue and the corresponding development of appropriate strategies for each situation. Growth factors are vital elements of tissue regeneration. Therefore, their convenient, effective and active forms should be delivered by appropriate scaffolds for an optimal recovery process. Since a broad range of growth factors exhibit an affinity towards GAGs, developing GAG-mimetic scaffolds or incorporating GAGs to the structure of scaffolds could be an effective approach for regulating and enhancing the regeneration process through their proper representation.

Direct delivery of growth factors has failed in clinical trials since the concentration of the growth factors needs to be above a threshold in order to show their effects on target cells. In addition, directly administered growth factors are more prone to degradation and may not reach the target area if injected intravenously or intramuscularly. As such, excessive doses of growth factors and several injections may be required for therapeutic effect. Increasing concentration of delivered growth factors may lead to undesirable consequences in case of angiogenic growth factors such as VEGF and FGF2, which can promote the development of pathological vessels and unbalance cellular dynamics to facilitate cancer formation [37, 38]. Therefore, unique and smart administration strategies need to be developed (Figure 4).

Natural and synthetic polymeric hydrogels are widely tested biomaterials due to their high hydration capacity and structural resemblance to the ECM. Physical entrapment or covalent placement of growth factors inside polymers may delay their denaturation and control their release profile thanks to the enhanced degradation kinetics of polymeric scaffolds [39]. Chemical immobilization of growth factors to polymers can be performed through covalent or non-covalent interactions. Non-covalent incorporation of growth factors into scaffolds can be performed through charged and hydrophobic group interactions or the addition of mediator molecules such as fibronectin, heparin or small oligopeptide sequences within the matrix structure. Fibrin networks are especially useful for this purpose, as they enhance clot formation and stop bleeding, in addition to easily encapsulating growth factors such as NGF or VEGF through their mesh-like structures and ECM-mimicking capabilities. Proteolytic degradation of fibrin by plasmin releases growth factors in a controllable manner and without losing their activity. As such, fibrin scaffolds have previously been used with

11

considerable success to enhance nerve regeneration (NGF) [40] and induce

angiogenesis (VEGF) [41].
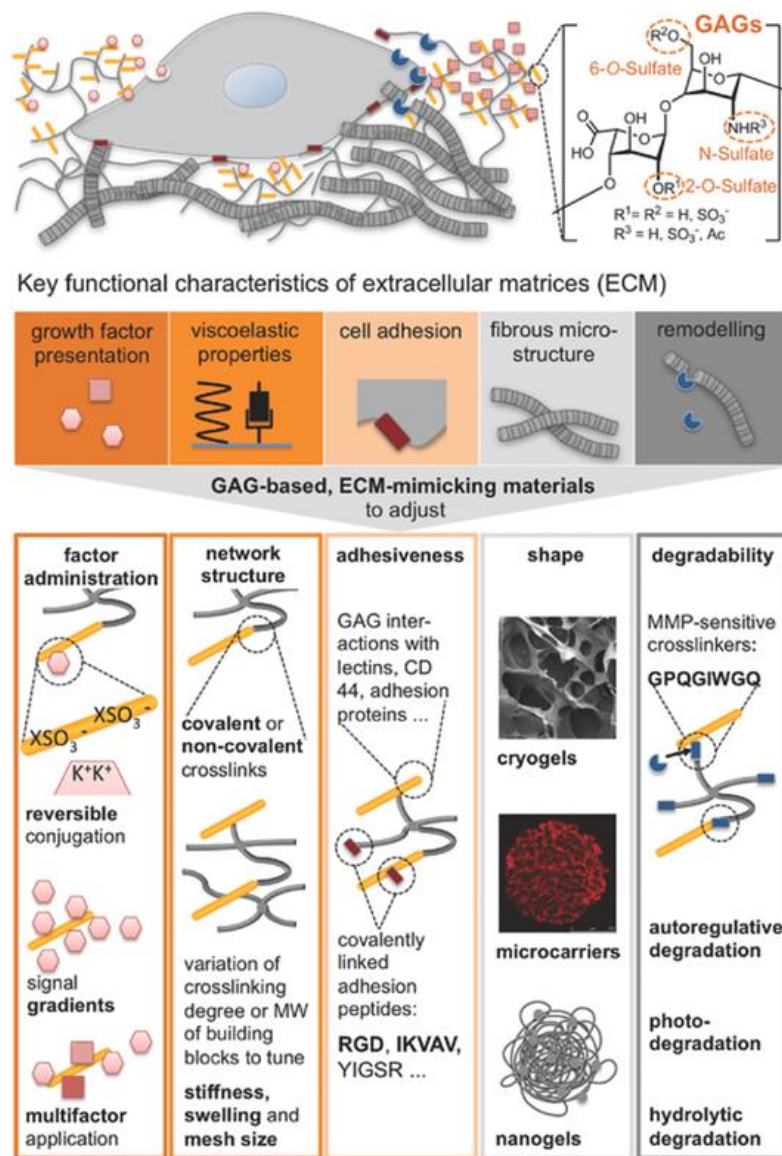
Figure 4: Properties of GAG-based, ECM-mimicking materials include the capacity

to deliver growth factors, provide a porous environment, create a platform for cell

adhesion and biodegrade naturally in the ECM. Copyrighted Advanced Materials,

Volume 28, Issue 40, October 26, 2016, DOI: 10.1002/adma.201601908 [1].

Combining ECM mimetic molecules and microporous polymers may also result in better regeneration. Conjugation of heparin to fibrin matrices has been investigated for the non-covalent loading of growth factors, and although NGF has a moderate affinity to heparin, heparin-loaded fibrin matrices were observed to facilitate the slow, controlled release of NGF and promote neurite extension [42]. In a similar way, loading of VEGF to alginate in conjunction with a covalently-attached cell adhesion peptide sequence enhanced the survival rate of endothelial cells and provided blood transmission to ischemic tissue [43]. In addition to natural polymers, synthetic polymers can also be used for growth factor release and exhibit some advantages such as ease of fabrication and chemical modification. For instance, encapsulation of VEGF to poly (d, l-lactide-co-glycolide) (PLG) polymer provides the sustained release of GF and enhances angiogenesis [44].

However, covalent interaction or encapsulation of growth factors to scaffolds may disrupt the active sites of GFs and interfere with their therapeutic effects. Interaction of growth factors with ECM components makes them spatiotemporally available and their association protects growth factors from degradation while providing their sustained release. Therefore, utilizing ECM components during the design of biomaterials could enhance the outcomes of growth factors delivery. It has been shown that heparin incorporation to poly (ethylene glycol) (PEG) with photo-crosslinkable vinyl epitopes promotes human mesenchymal stem cell (hMSCs) proliferation due to the sustained release of FGF-2 [45] and, additionally, three dimensional culturing could be used to induce the osteogenic differentiation of hMSCs through the use of the heparin binding molecules BMP-2 and fibronectin [46]. These systems were also able to facilitate the slow release of their contents, as an FGF-2 release from gels consisting

13

of heparin/hyaluronan and heparin/CS combinations (which were conjugated to PEG diacrylate through the thiol modification of GAGs) was significantly slower than gels without heparin. In addition, subcutaneous injection of FGF-2-loaded heparin and GAG combined hydrogels promoted blood vessel formation due to the sustained release of FGF-2 [47]. Another strategy for heparin mobilization to hydrogels was developed by Mizushima *et al.*, who used an ethylenediamine linker to crosslink carboxylates of heparin to carboxylates of alginate. The heparin-alginate hydrogel decreased the release rate of FGF-2 *in vitro* and FGF-2 loaded hydrogel implantation to the dorsum of rats significantly enhanced angiogenesis [48]. Overall, both natural and synthetic ECM-mimetic scaffolds are highly promising for tissue regeneration studies due to their ability to enhance the sustained release of growth factors while protecting them from degradation.

1.4. Self-Assembled Peptide Nanofiber Networks for Regenerative Medicine

Regeneration of tissues requires dedicated bioactive signaling networks to form fully functional and desired the type of tissue. Supramolecular materials are generated to interact with each other through non-covalent intermolecular bonds depending on environmental stimuli. These biomaterials satisfy the strict requirements of tissue regeneration processes by providing appropriate signals in a controllable manner, exhibiting the ability to adjust their mechanical properties and being degraded without toxicity after completing their mission. Self-assembling peptide hydrogels are next-generation biomaterials for tissue engineering applications and offer biocompatible, biodegradable and bioactive epitope bearing networks that mimic the ECM of cells and thereby support their proliferation, adhesion, and migration [49].

Self-assembled systems are produced by two main approaches: (a) the extension of oligomeric chains and crosslinking of the resulting polymeric molecules and (b) self-assembly of monomeric molecules such as peptide amphiphiles and aromatic group-edited oligopeptides (Figure 5). Self-assembly is driven by noncovalent interactions such as electrostatic interactions, hydrogen bonding or hydrophobic interactions [50]. Bioactive sequence-edited polymers supply ECM mimetic porous, fibrous environments to cells while directing their responses by providing the proper signals for healing. As an example of self-assembled peptide and polymer hydrogels, Stupp and co-workers designed starPEG-peptide-HEP (heparin) hydrogels that present sequences derived from the bioactive molecules of ECM, such as IKVAV (laminin-1- derived) and RGD (derived from fibronectin). These hydrogels were demonstrated to effectively facilitate the spreading and elongation of HUVECs, as well as the neurite outgrowth of dorsal root ganglia [51]. Peptide nanofiber systems provide an opportunity to easily present a precise set of bioactive epitopes depending on the type of damaged tissue. For example, the induction angiogenesis was facilitated by a heparin-binding sequence (LRKKLGKA) containing peptide amphiphile (heparin-PA) and heparin nanofibers in a rat corneal assay [52]. Further, heparin-PA nanofibers have been found to promote extensive revascularization in a chronic rat ischemic hind limb model [53]. The addition of growth factor-binding sequences to self-assembled nanofibers can also enable the sustained and efficient delivery of growth factors and encourage the regeneration of damaged tissues. Stupp and co-workers, for example, designed and synthesized peptide amphiphiles (PA) containing a BMP-2 binding sequence (NH$_2$–TSPHVPYGGGS–COOH) and demonstrated that the injection of this PA molecule with low doses of BMP-2 (100 ng) led to spinal fusion in rats [54].
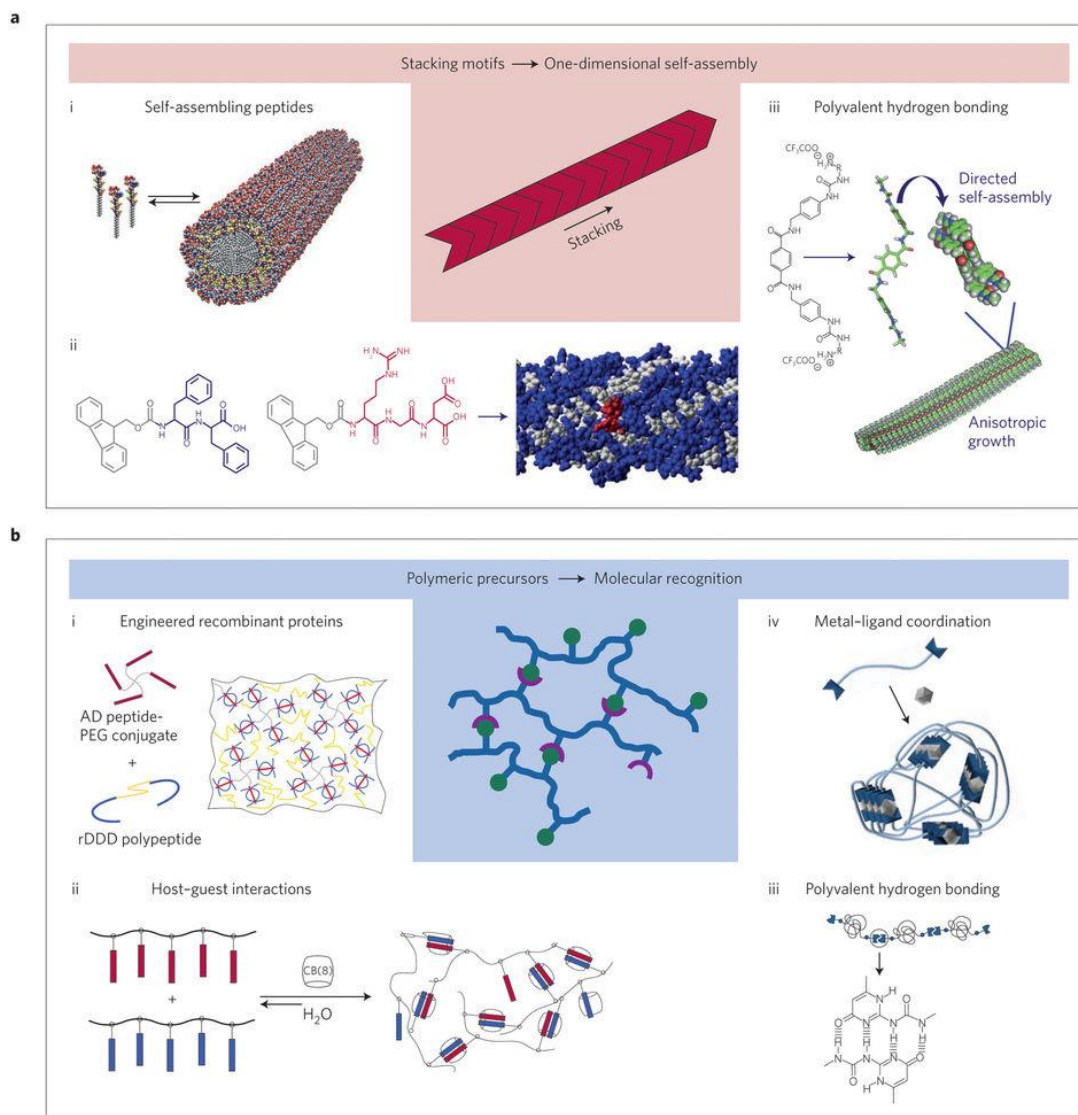
Figure 5: An overview of supramolecular interactions. a) Stacking motifs create one-dimensional self-assembled structures such as i) peptide amphiphiles and ii) aromatic group-containing oligopeptides; iii) which gather and self-assemble through hydrogen bonding and hydrophobic interactions. b) Formation of polymeric supramolecular biomaterials through molecular recognition strategies; i) cross-linking by recognition of the docking domain by polymer-conjugated engineered recombinant proteins; ii) Crosslinking through host-guest affinity; iii) elongation of oligomeric precursor through hydrogen-bonding; iv) metal-ligand interaction-facilitated oligomer extension. Copyrighted by Nature Materials 15, 13–26 (2016) doi:10.1038/nmat4474 [50].

16

Since many of the growth factors have heparin-binding domains, the design of heparin mimetic peptide nanofibers could be highly effective for a range of regenerative medicine applications. Previously, our group designed and synthesized heparin-mimetic (HM) peptide nanofibers (lauryl-VVAGEGDK(p-benzosulfonate)S-Am) that exhibited the ability to induce angiogenesis *in vitro* and *in vivo* [55]. Further investigation of the angiogenesis induction mechanisms of HM peptide nanofibers revealed that HM peptide nanofibers interacted with VEGF and FGF-2 molecules and promoted angiogenesis even in the absence of external growth factor addition by concentrating and presenting endogenously produced growth factors. In addition, although NGF has a moderate affinity towards heparin, HM-peptide nanofibers supported neurite outgrowth of PC12 cells, which suggests that NGF attached to HM peptide nanofibers and exerted its effects without losing its bioactivity [56]. The capacity of HM peptide nanofibers to induce angiogenesis was also confirmed through *in vivo* applications, and is peptide system was able to enhance the healing of acute wounds [57], shorten recovery times in burn wounds [58], support and increase the functionality of pancreatic islet transplantation [59], and assist in the repair of cardiac tissue /degeneration after myocardial infarction [60]. Additionally, chondrogenesis-promoting potential of HM peptide nanofibers was indicated by the growth and differentiation of prechondrogenic cells [61]. Furthermore, HM-peptide nanofibers supported the mineralization of osteoblast-like cells [62] and led bone regeneration and mineralization in a rabbit tibial bone defect model [63]. Thus, mimicking glycosaminoglycans by self-assembled peptide nanofiber networks is a promising approach in many areas of tissue engineering.

Chapter 2

2. AFFINITY OF GLYCOPEPTIDE NANOFIBERS TO GROWTH FACTORS AND THEIR EFFECTS ON CELLS

2.1.   Introduction

Regeneration of tissues requires the coordinated action of a complex network of signaling molecules between intracellular, intercellular and extracellular environments. Growth factors are one of the essential components of the regeneration process, and their activity patterns depend on the type of tissue [64]. Appropriate presentation of growth factors at the site of injury has been shown to enhance the regeneration of skin, [47, 65] bone [66] and cartilage [67] tissues. Non-covalent growth factor localization strategies, such as glycosaminoglycan and proteoglycan integration to scaffolds [52, 68] or covalent immobilization of growth factors to biomaterials [69, 70], have been considerably successful in directing and manipulating the fate of cells and recently emerged as a preferred approach for tissue regeneration. However, complications associated with the direct introduction to growth factors to delivery sites, such as burst release, rapid degradation of growth factors [64] within scaffolds, steric hindrance of active sites during receptor recognition, loss of native growth factor conformation, and limited internalization of growth factor-receptor complexes due to improper covalent interactions, complicate the use of growth factors for mediating wound recovery [71]. Therefore, smart and controllable growth factor release platforms that mimic growth factor-affine structures would be promising candidates for regeneration.

The present chapter describes the design and synthesis of a glycopeptide nanofiber array containing four monosaccharide epitopes: glucose, N-acetylglucosamine, galactose, and mannose. These GAG-inspired, growth factor-affine nanostructures were tested for their ability to present growth factors for tissue regeneration through binding assays for the heparin-binding growth factors VEGF and FGF-2, as well as the non-heparin-binding growth factor NGF.

2.2. Experimental Section
2.2.1. Materials

9-Fluorenylmethoxycarbonyl (Fmoc) and tert-butoxycarbonyl (Boc) protected amino acids, lauric acid, 2-(1H-benzotriazol-1-yl)-1,1,3,3-tetramethyluronium hexafluorophosphate (HBTU), 4-(2′,4′-dimethoxymethyl-Fmoc-aminomethyl)-phenoxyacetamido-norleucyl-MBHA resin (Rink amide MBHA resin) and diisopropylethylamine (DIEA) were supplied from Merck and all other chemicals were purchased from Sigma-Aldrich, Thermo Scientific, Invitrogen, and Fisher.

2.2.2. Synthesis of Purification of Amphiphilic Glycopeptides

Glucose-, galactose-, mannose- and N-acetylglucosamine-bearing PA molecules were synthesized by solid phase peptide synthesis method. All carbohydrate residues have been functionalized into allyl glycosides and then converted to carboxylic acid derivatives, which could be easily attached to the side chain amine group on the resin-bound PA. Allyl glycoside can be synthesized by various glycosidation methods depending on the carbohydrate; in this work, $BF_3.Et_2O$ was used for glucose, mannose and N-acetylglucosamine PAs while the Koenigs-Knorr reaction silver carbonate (Ag_2Co_3) was used for galactose PA. We have attached the above-mentioned carbohydrate carboxylic acid to the glutamic acid-containing PA using the standard amino acid coupling agent HBTU/DIPEA on a solid phase. C_{12}-VVAGEK (Mtt) was synthesized on peptide synthesizer and then Mtt group was cleaved to produce free amines for coupling the carbohydrate carboxylic acid derivative. After successful coupling of the carbohydrate, deprotection of the acetate group was also performed on solid phase using 10% hydrazine in DMF under overnight shaking. Glycopeptide was cleaved from the solid support using peptide cleavage cocktail (TFA:TIS:H_2O,

95:2.5:2.5). A similar synthetic procedure is applied for the synthesis of all other Glyco-PAs. Characterization of PAs was performed by using an Agilent liquid chromatography-mass spectrometry (LC-MS). The crude Glyco-PAs were purified by using An Agilent 1200 preparative reverse-phase HPLC 0.1% (NH_4OH) in acetonitrile and water as mobile phase gradient. After the HPLC, acetonitrile was removed on rotary evaporator and then samples were lyophilized to get pure Glyco-PAs.

2.2.3. Physical and Chemical Characterization of Peptide Amphiphiles

2.2.3.1. Scanning Electron Microscopy (SEM) Imaging

Glycopeptide nanofibers were prepared by mixing monosaccharide PA and K-PA (at a 1:0.33 and 1:1 molar ratios) and, for sulfated systems, monosaccharide PA, SO_3-PA and K-PA (at a 1:1:0.65 molar ratio). Mixed glycopeptide nanofibers (1 wt%) on silicon wafers were incubated at 37 ℃ for 30 min and gradually dehydrated with 20, 40, 60, 80 and 100% ethanol. Samples were critical point-dried using an Autosandri-815B CPD equipment (Tousimis). Critical point-dried samples were sputter-coated with 9 nm of gold-palladium and imaged under a beam energy of 30 keV using an FEI Quanta 200 FEG SEM system.

2.2.3.2. Atomic Force Microscopy (AFM) Imaging

Glycopeptide nanofibers (under the same combinations for SEM imaging) were air-dried on glass slides and imaged under contact made using SiNi cantilevers using an Asylum Research MFP-3D atomic force microscope. A scan rate of 0.5 Hz was used for all images. 5 μm x 5 μm topographs were acquired for each sample at a pixel resolution of 512 x 512.

2.2.3.3.   Circular Dichroism (CD) Analyses

A J-815 Jasco CD spectrophotometer was utilized to determine the secondary structures of peptide nanofibers at room temperature. Stock solutions of each PA were dissolved inside water at 1 mM concentration and mixed with oppositely charged K-PA. For CD spectroscopy measurements, peptide nanofibers were diluted to 0.25 µM. Measurements were carried out in the range of 300 nm to 190 nm with 100 nm/min scanning speed. Bandwidth was adjusted to 1 nm while data pitch and data interval were set as 0.1 nm. Digital integration time was chosen as 1 s at standard sensitivity. The molar ellipticity of each nanofiber system was calculated using three replicate measurements.

2.2.4. Affinity of Growth Factors to Peptide Nanofibers via ELISA- Binding Assay

The affinity of VEGF, FGF-2, and NGF to peptide nanofibers was analyzed using ELISA. Each glycopeptide amphiphile was mixed with positively-charged K-PA (C_{12}-VVAGK) (1:0.33 molar ratio of VEGF and FGF2 molecules and 1:1 molar ratio for NGF molecule) inside wells (Maxisorp, NUNC-Immuno plate, Thermo Scientific). Additionaly, glycopeptide – sulfonate peptide amphiphile (C_{12}-VVAGE (K-p-sulfobenzoate) - K PA (1: 1: 0.65 molar ratio) combinations were prepared and tested against VEGF and FGF2. Wells were coated with peptide nanofibers (3 wells per each group) and dried overnight inside a laminar flow hood. Dried peptide nanofibers were washed thrice with wash buffer and tapped for drying. Assay buffer was added to each well for blocking. After the washing and drying of wells, growth factor was added to wells and incubated overnight at +4 ºC. On the next day, ELISA plate was incubated

at room temperature for 30 min and washed five times with wash buffer. After tapping and drying steps, a biotinylated antibody of growth factor was added to wells. Detection of biotinylated antibody was carried out with horseradish peroxide (HRP) conjugated streptavidin molecule. 3, 3' 5, 5'– tetramethylbenzidine (TMB), the substrate of HRP, was added and incubated for 15-20 min. To finalize the reaction, stop solution (sulfuric acid) was added and the absorbance at 450 nm wavelength was measured by a microplate reader (Spectramax M5). Absorbance at 600 nm wavelength was taken as the reference point for calculations.

2.2.5. Live-Dead Assay- Cellular Viability Analyses

Biocompatibility of human umbilical vein endothelial (HUVEC) and PC-12 (ATCC® CRL-1721™) cells cultured on peptide nanofibers was tested by Live/Dead Assay. Peptide nanofibers were coated on 96 well plates (n=3). After 24 h and 48 h of incubation, plates were centrifuged at 2500 rpm for 5 min, washed with PBS and centrifuged at 2500 rpm for 1 min. Calcein-AM (which stains live cells) and ethidium homodimer-1 (which stains dead cells) were added to wells at concentrations recommended by the manufacturer. Five photos from each well for each group were taken by fluorescence microscopy (ZEISS Axio Observer A1) and counted using the Image J cell counter software.

2.2.6. Tube Formation Assay

In vitro tube formation assay was carried out by coating each glycopeptide - K-PA (1:0.33 molar ratio) and glycopeptide-sulfonate - K-PA (1:1:0.65 molar ratio) nanofibers on 96 well plates and drying peptide combinations overnight in a laminar flow hood. On the next day, HUVECs were trypsinized and counted with a

hemocytometer. 5 x 10^4 cells/well were seeded inside 1% fetal bovine serum (FBS) containing low glucose DMEM and incubated for 36 h. Five photos from each well for each group were taken by ZEISS Axio Observer A1 microscope and the length of tubular structures was quantified by Image J software.

2.2.7. Neurite Extension Assay

Glycopeptide/K-PA (1:1 molar ratio) nanofibers were coated to well plates (3 wells for each group). After overnight drying, PC12 cells were seeded in expansion medium (RPMI with 10% horse serum (HS), 5% FBS and 1% penicillin/streptomycin (P/S)). On the next day, medium was changed with differentiation medium (MEM with 2% HS, 1% FBS, 1% P/S) with additional NGF (20 ng/mL). Five photos from each well for each group were taken by ZEISS Axio Observer A1 microscope at the end of the six-day incubation. Lengths of extended neurites were quantified by Image J software.

2.2.8. VEGF and FGF-2 Secretion Analysis

Secretion of VEGF and FGF-2 from HUVECs cultured on glycopeptide/K-PA (1: 0.33 molar ratio) and glycopeptide/sulfonate/K-PA (1: 1: 0.65 molar ratio) nanofiber systems were analyzed with ELISA at four-time points; 12 h, 24 h, 36 h and 48 h. VEGF and FGF-2 coating antibodies, AHG9119D (Invitrogen) and MAB233 (R&D Systems) respectively, were coated to Maxisorp ELISA plates and incubated overnight at +4 ºC. On the next day, blocking of wells was performed with assay buffer. For each time point, supernatants of each group were collected and added to antibody-coated wells and incubated overnight at +4 ºC. On the next day, biotinylated antibodies, streptavidin-HRP, TMB and stop solution were added to wells one by one.

Absorbances at 450 nm wavelength were read by taking the 600 nm wavelength as a reference point using a microplate reader (Spectramax M5).

2.2.9. Statistical Analysis

One-way analysis of variance (ANOVA) with Tukey's post-tests was carried out for each experimental setting using GraphPad Prism 6 software. Standard errors of the means were represented in graphics. $p < 0.05$ was accepted as statistically significant.

2.3. Results and Discussion
2.3.1. Synthesis and Characterization of Glycopeptide Nanofibers

Glycopeptide amphiphiles (glucose, galactose, mannose and N-acetylglucosamine PAs), sulfonate-PA, E-PA, and K-PA were synthesized by solid phase peptide synthesis method and their purities were validated by LC-MS (Figure 6, 7, 8, 9). Each glycopeptide had different monosaccharide units and N-acetyl-glucosamine-PA was synthesized because one of the saccharide units of GAGs is an acetylated amino sugar. Additionally, sulfonate-PA-including combinations were designed in order to obtain much more similar structures to GAGs. E-PA was used as the non-bioactive PA control group since it does not have any saccharide group. Nanofiber networks were formed by mixing with oppositely-charged K-PA. Each peptide pH was adjusted to physiological pH ($\approx$ 7.4) before the formation of the nanofiber networks. GAG-mimetic nanofibers were adjusted to have a highly negative charge to better imitate natural GAG networks through the addition of K-PA at a lower molarity. This system was used for VEGF and FGF-2 interaction studies. Since NGF does not have a heparin binding domain, the NGF affinity of glycopeptide and K-PA nanofiber systems was determined using peptide mixtures containing each component at the same molarity. All individual PA molecules were analyzed by CD spectroscopy in order to confirm that β-sheet structure is only observed following interaction with the oppositely charged K-PA, and we did not observe a β-sheet signal in this case (Figure 10). For each condition, the constituted nanofiber systems were analyzed by CD spectroscopy in order to determine their secondary structures. A positive peak around 200 nm and a corresponding negative peak around 220 nm are indicators of β-sheet formation, which is also a sign of nanofiber formation in each system (Figure 11). Self-assembled nanofibers were further visualized by AFM imaging, and height maps of each system

26

were found to indicate nanofiber formation (Figure 12). SEM imaging of glycopeptide nanofiber systems demonstrated an ECM-like porous fibrous network formation for each combination (Figure 13, 14).
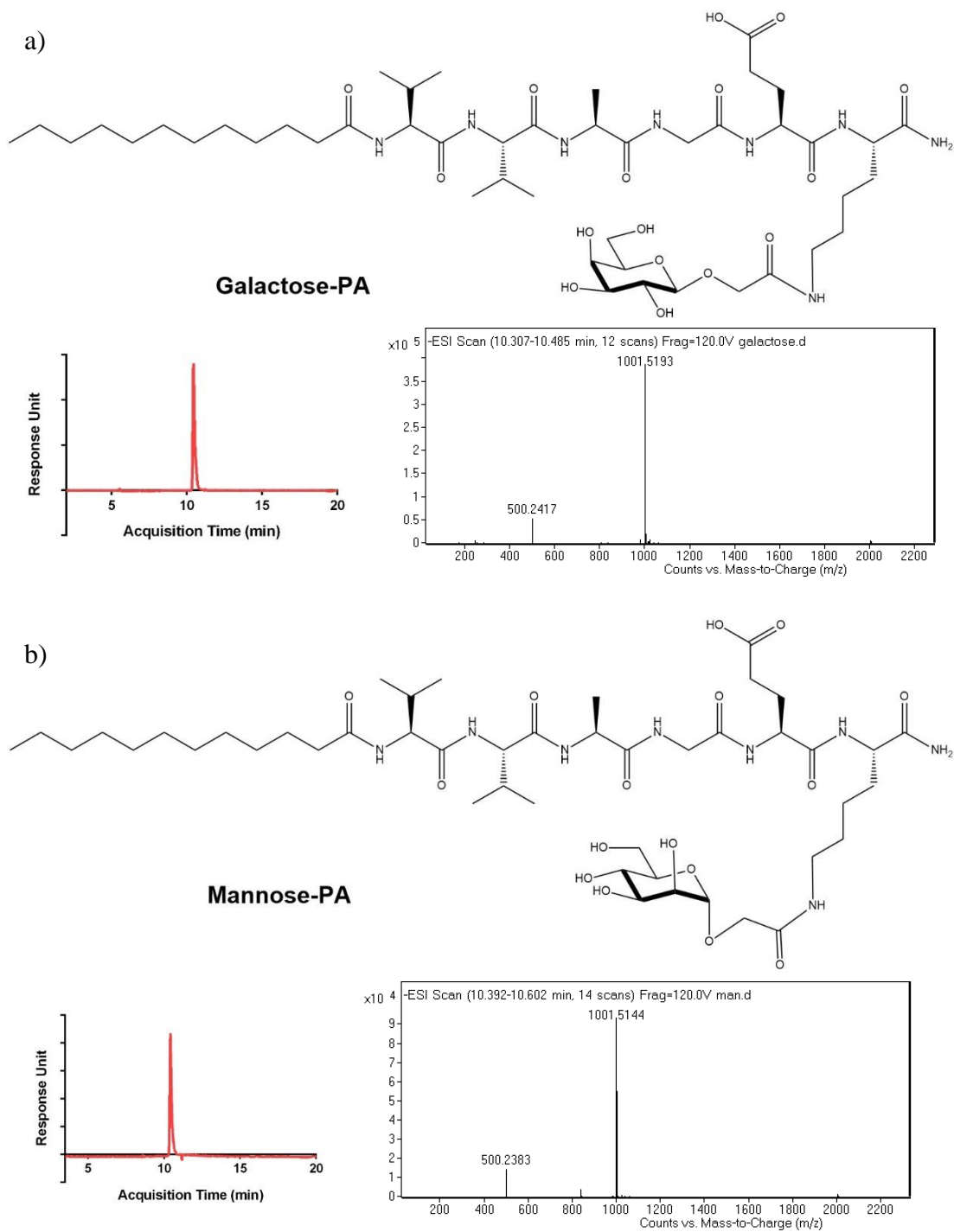
Figure 6: Chemical structures and LC-MS analyses of a) galactose-PA and b) mannose-PA.

a)

Glucose-PA

x10 4 -ESI Scan (10.363-10.654 min, 19 scans) Frag=120.0V glucose.d
1001,5201
500.2413

b)

N-acetylglucosamine-PA

x10 6 -ESI Scan (10.315-10.654 min, 22 scans) Frag=120.0V nac.d
1042,5335
520.7462
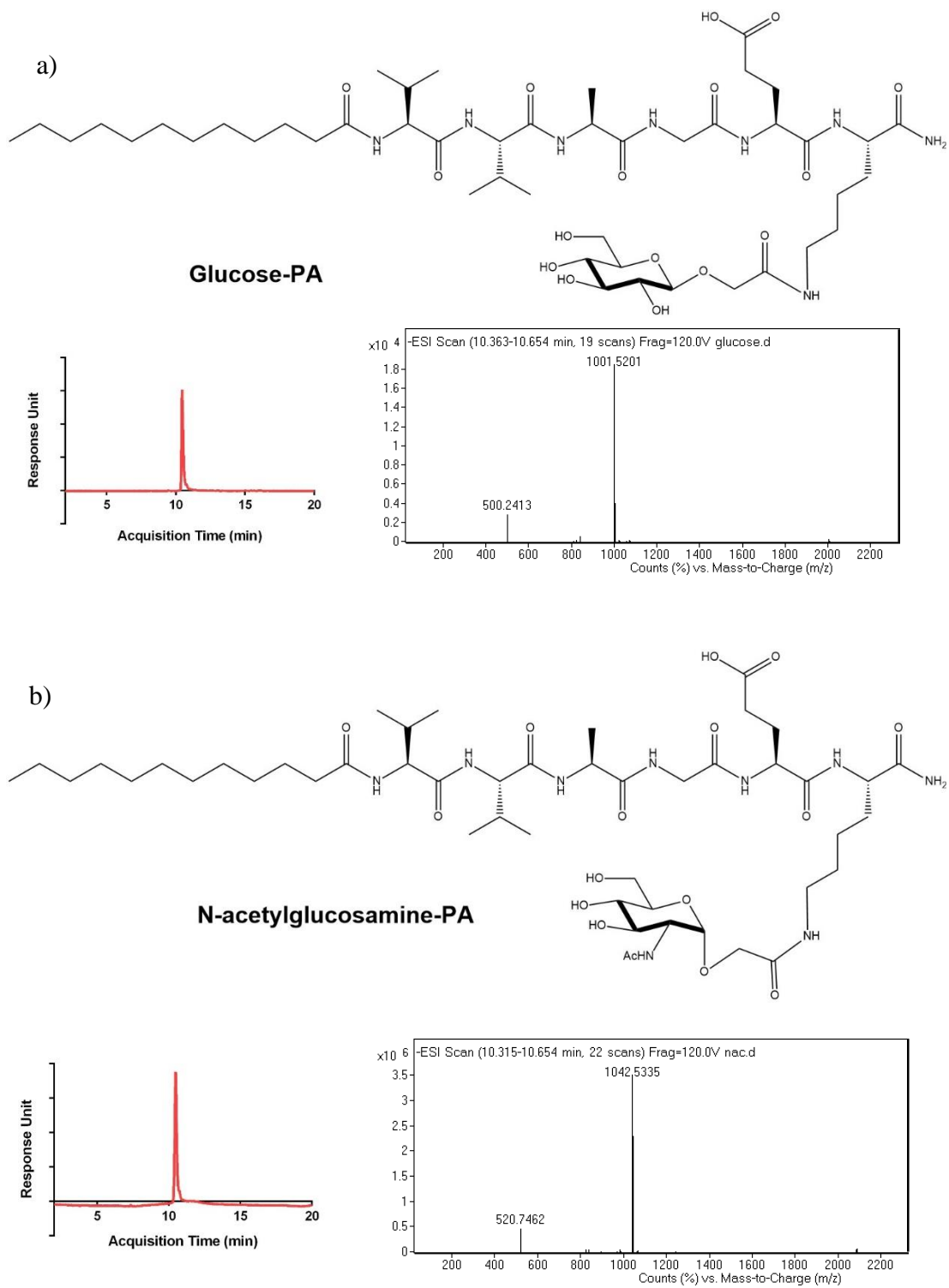
Figure 7: Chemical structures and LC-MS analyses of a) glucose-PA and b) N-acetylglucosamine-PA
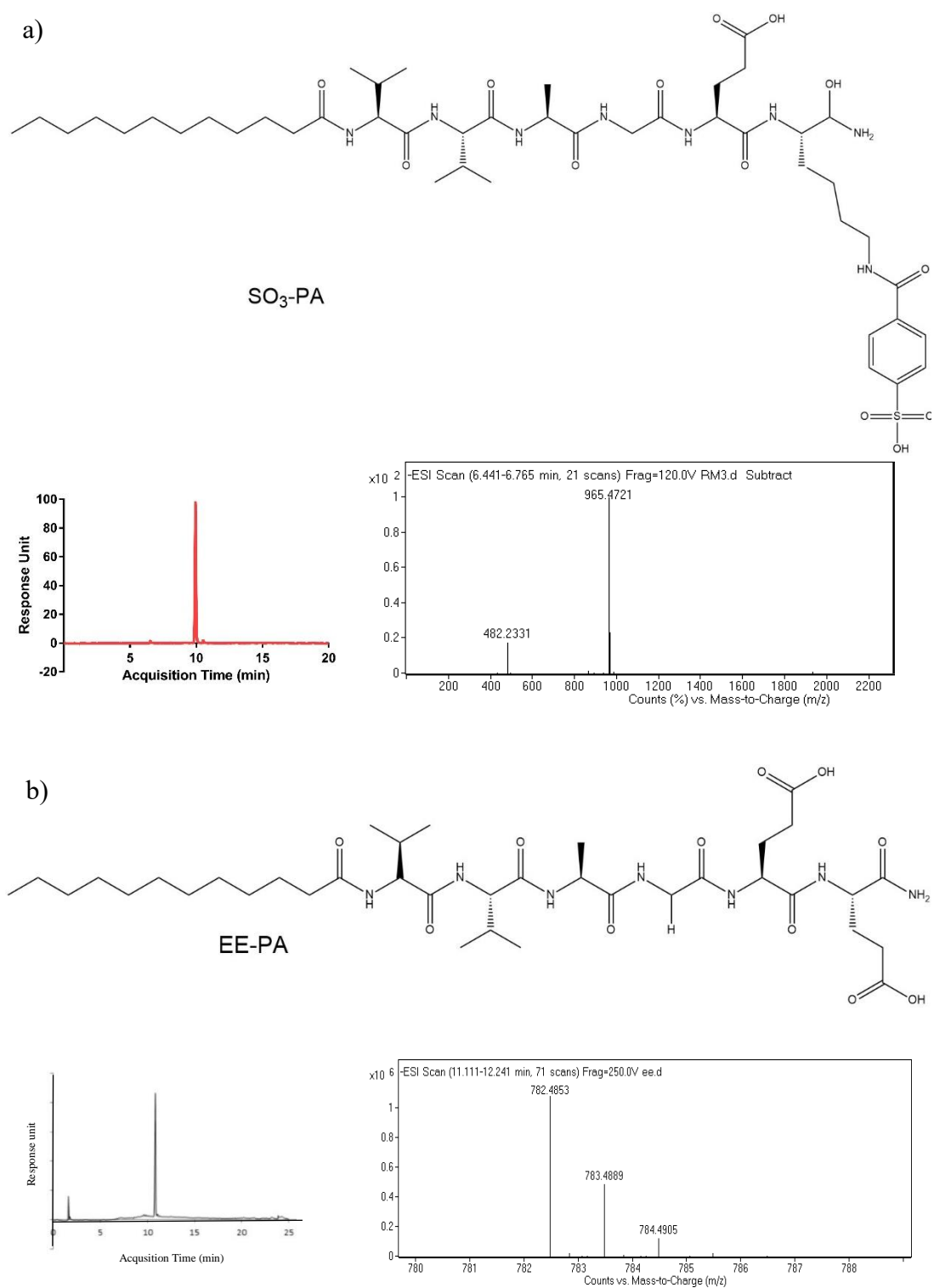
Figure 8: Chemical structures and LC-MS analyses of a) SO₃-PA and b) EE-PA.

K-PA
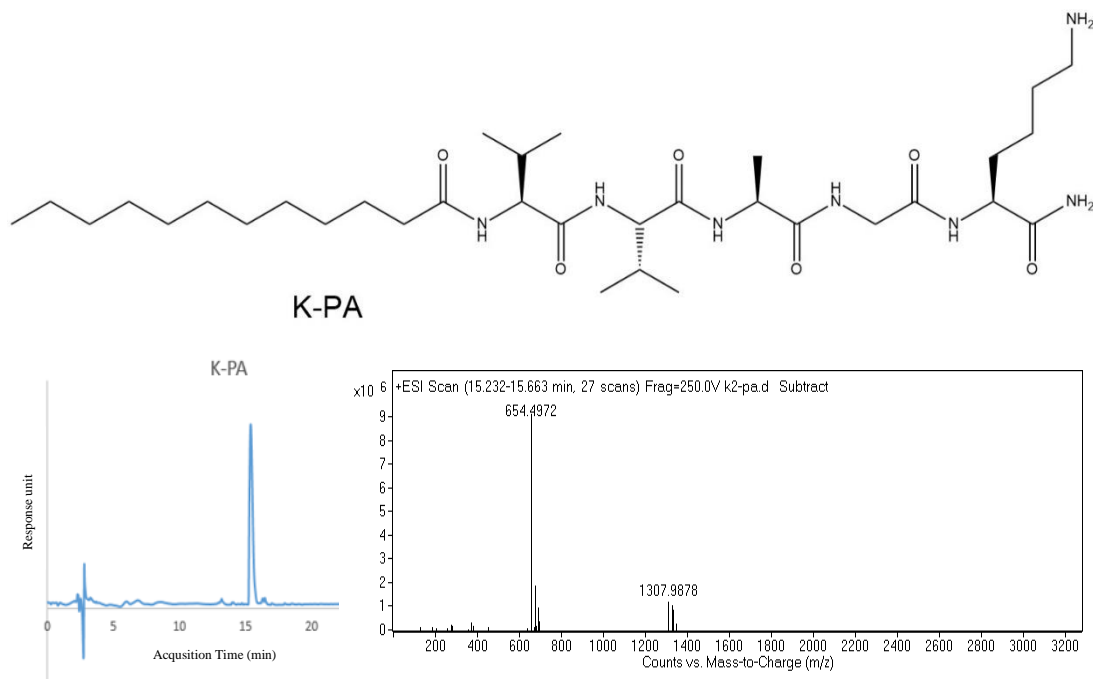
Figure 9: Chemical structure and LC-MS analyses of K-PA.
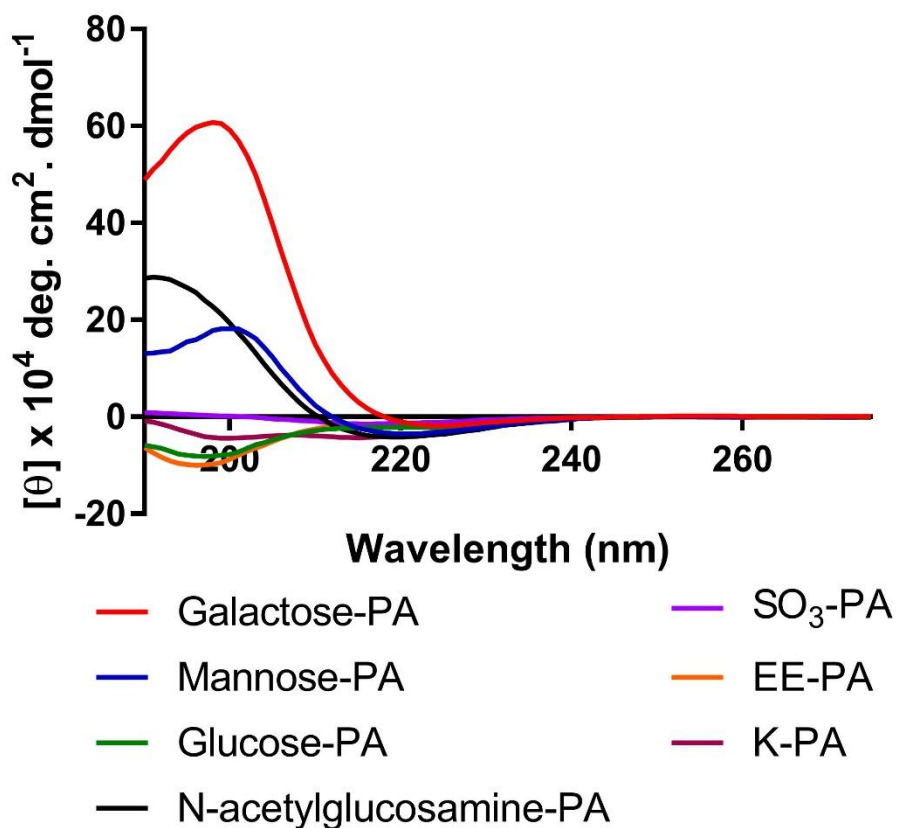
Figure 10: CD spectra analyses of peptide amphiphile molecules.
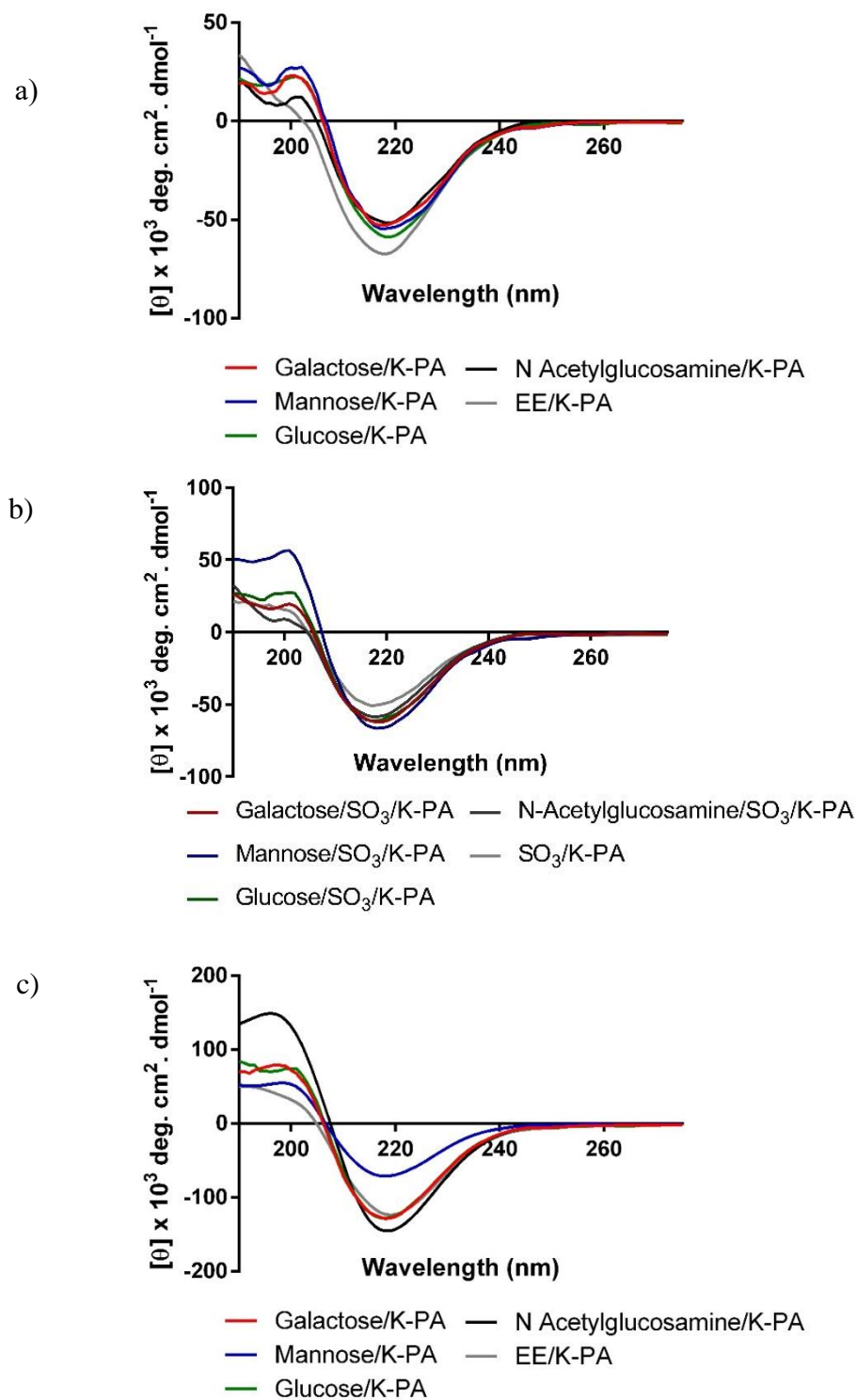
Figure 11: CD spectra of glycopeptide nanofibers that are formed by the addition of the oppositely charged K-PA. a) Only glycopeptide and K-PA combinations; b) Glycopeptide/sulonfate PA and K-PA combinations and c) Equimolar glycopeptide/K-PA combinations that were analyzed for NGF binding
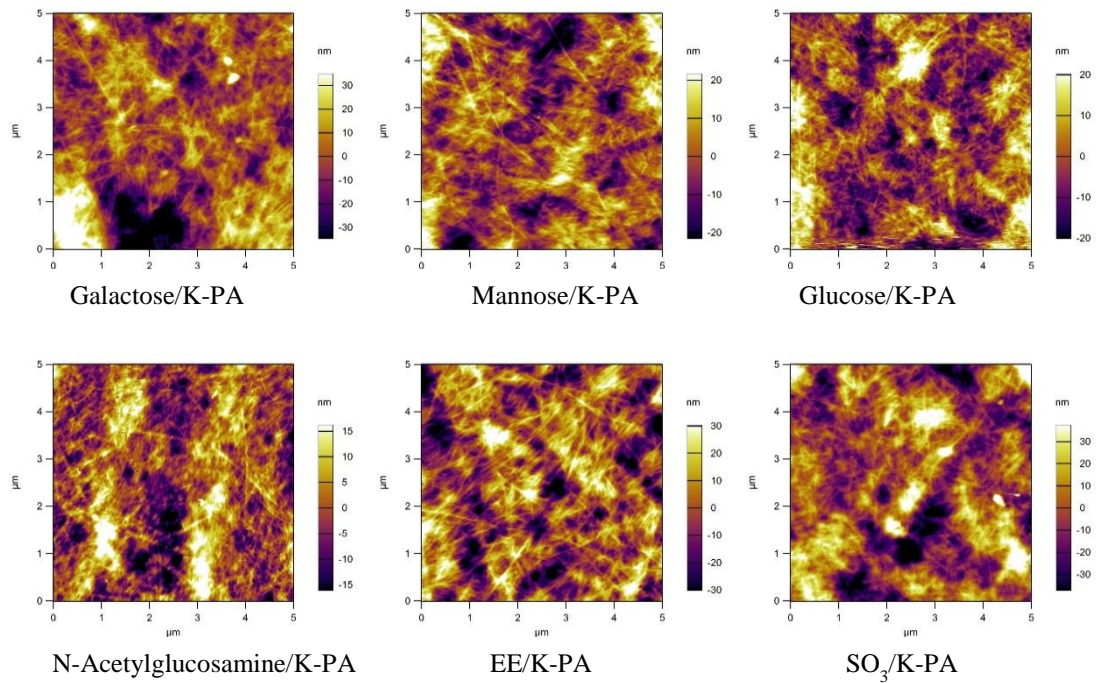
Figure 12: Height maps of glycopeptide nanofibers.
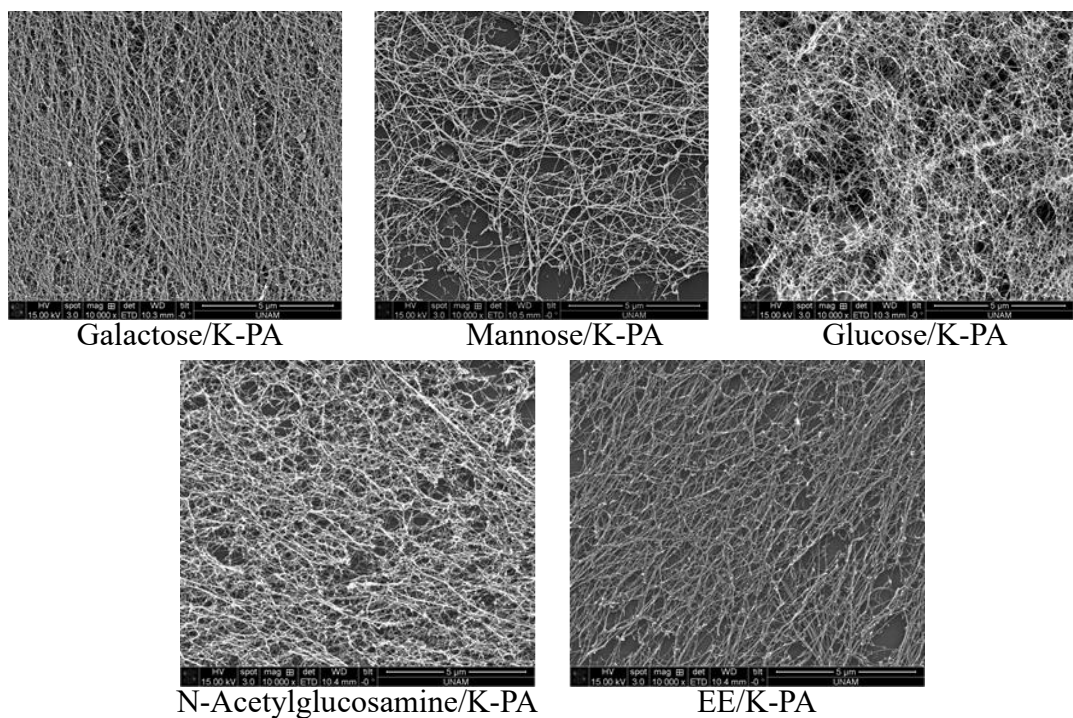
Figure 13: SEM imaging reveals the ECM-like nanofibrous, porous network of glycopeptide nanofibers. (Combinations for NGF binding)

Galactose/K-PA   Mannose/K-PA   Glucose/K-PA

N-Acetylglucosamine/K-PA   EE/K-PA

Galactose/SO$_3$/K-PA   Mannose/SO$_3$/K-PA   Glucose/SO$_3$/K-PA

N-Acetylglucosamine/SO$_3$/K-PA   SO$_3$/K-PA
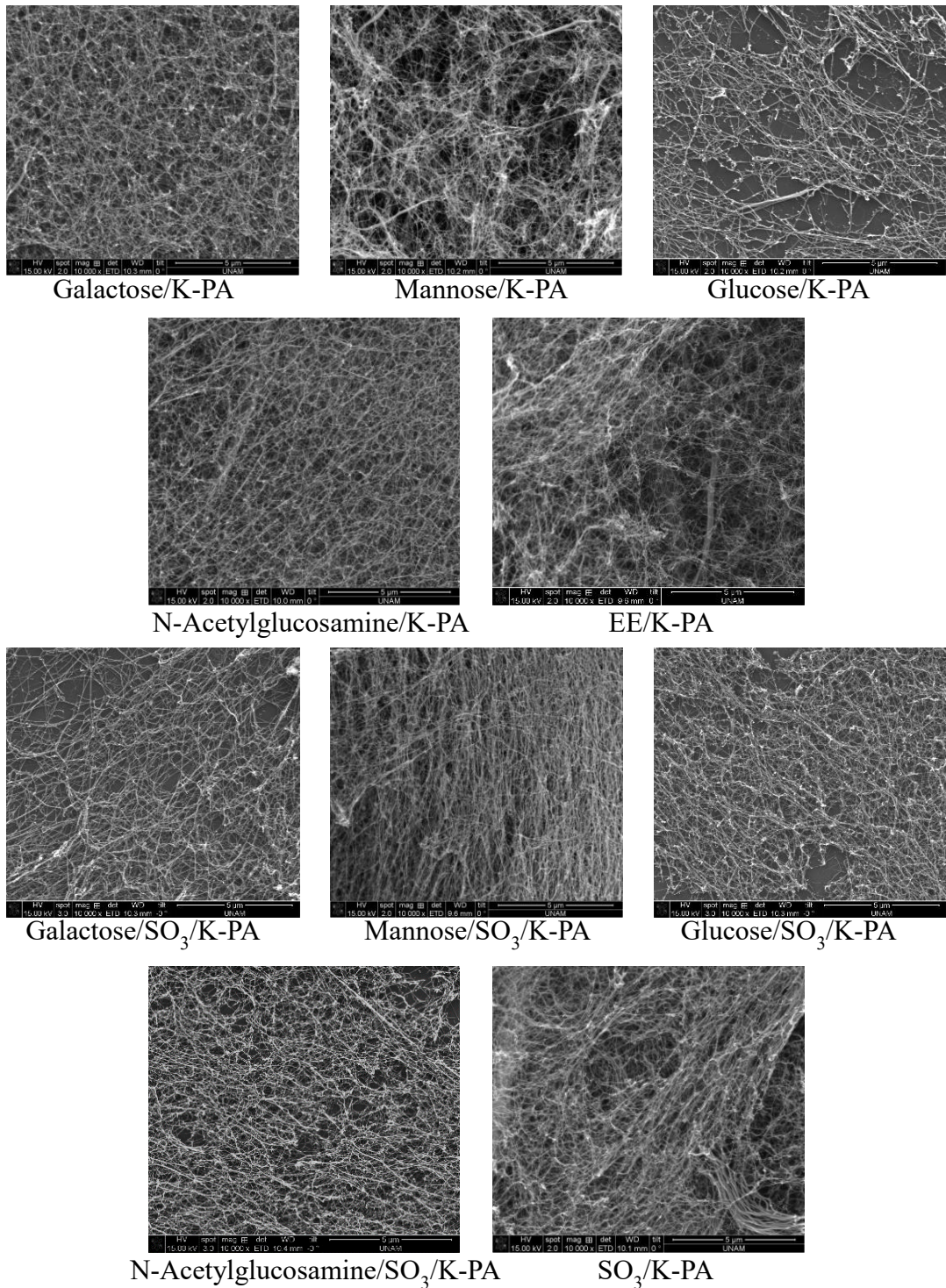
Figure 14: SEM imaging reveals the ECM-like nanofibrous, porous network of glycopeptide nanofibers. (Combinations for VEGF and FGF 2 binding)

2.3.2. Affinity Analysis of Growth Factors to Glycopeptides

The Affinity of glycopeptide nanofibers to VEGF, FGF-2 and NGF molecules were analyzed by ELISA method. Galactose and mannose nanofibers showed higher absorbance than glucose and N-acetylglucosamine nanofibers. However, EE/K-PA nanofiber (glutamic acid-bearing nanofiber) had a higher affinity to VEGF and FGF than non-mixed glycopeptide nanofibers. Since the EE/K-PA nanofiber has two carboxyl groups in its chemical structure, it is likely to be exhibit more electrostatic activity inside the buffer environment and effectively bear a greater negative charge than glycopeptides, although total charges of the nanofiber systems were equal. Since glycosaminoglycans consist of sulfated forms of sugars, SO_3-PA was also incorporated into the nanofiber systems. The addition of sulfonate PA to glycopeptides significantly enhanced VEGF and FGF-2 binding to nanofibers. In particular, sulfonate-added galactose, mannose and glucose nanofibers bound to VEGF significantly higher than the N-acetylglucosamine- SO_3 nanofiber (Figure 14a). It has been shown that VEGF interaction with HS is mediated through carboxylate groups and the 2-O, 6-O and N-sulfation of the HS chain [83]. Therefore, the lower affinity of N-acetylglucosamine-sulfonate nanofibers could result from the incompatibility of the spatiotemporal positions of sulfonate and N-acetylglucosamine groups on the surface of nanofibers for VEGF binding.

The addition of SO_3-PA to glycopeptides also increased FGF-2 binding to mannose and glucose glycopeptides. However, SO_3 PA-added galactose and N-acetylglucosamine glycopeptides showed the lower binding capacity to FGF-2 (Figure 14 b). Since total negative charge and length of HS is important for FGF-2 binding,

the assembly of mannose-sulfonate, glucose-sulfonate and sulfonate nanofiber combinations may present more negative epitopes on the surface of nanofibers.
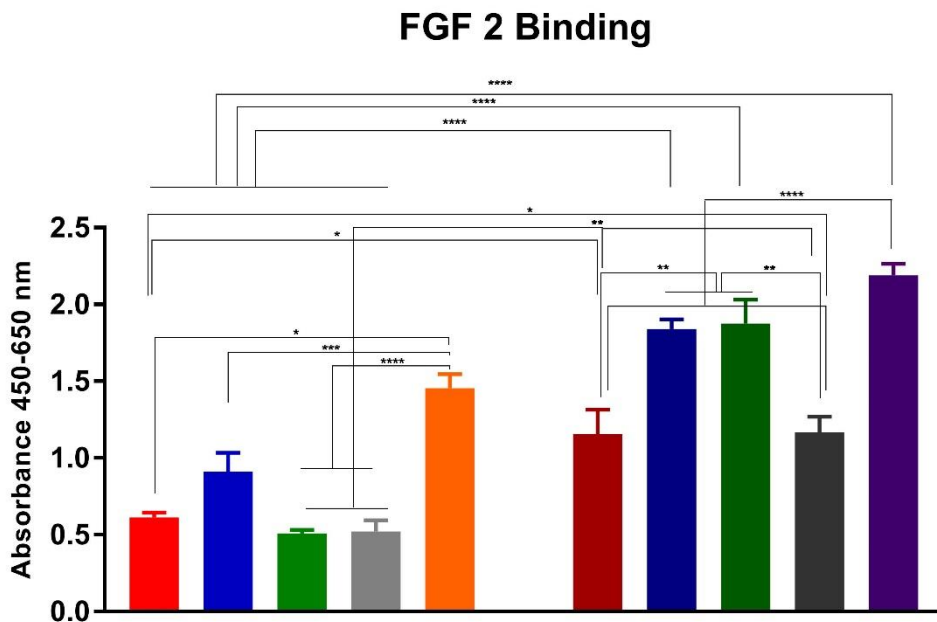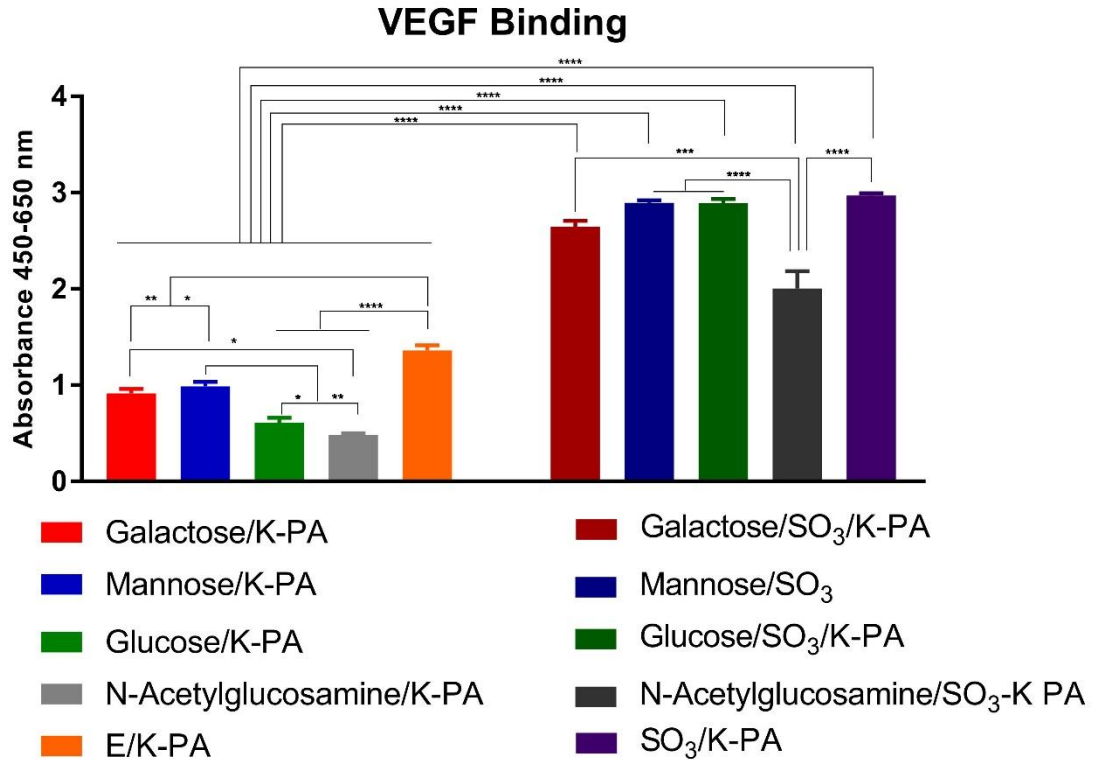
Figure 15: a) VEGF affinity to glycopeptide and glycopeptide-sulphate nanofiber network. b) FGF-2 affinity to glycopeptide and glycopeptide-sulfonate nanofiber network. Values represent mean ±SEM (****$p < 0.0001$).

The entire glycopeptide array was also investigated to determine whether monosaccharides had any affinity to NGF. Since NGF has moderate affinity against sulfated GAGs, only saccharide-bearing peptide nanofibers were investigated for the charge-neutralized combinations of glycopeptides and K-PA. ELISA results indicated that all monosaccharide bearing peptide nanofibers had high affinity to NGF (Figure 15). Therefore, glycopeptide nanofibers could be used as sustained NGF-secreting scaffolds for peripheral nerve regeneration studies.
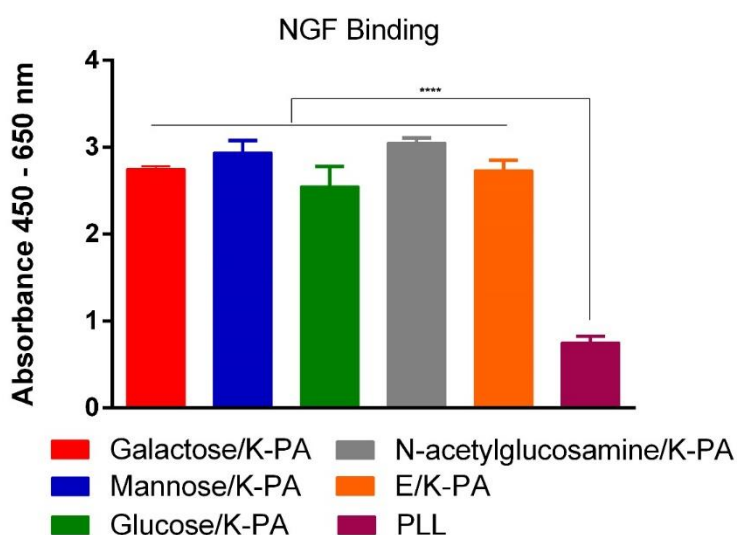
Figure 16: NGF affinity to glycopeptide nanofibers. Values represent mean ± SEM (****$p<0.0001$).

2.3.3. Viability of Cells on Glycopeptide Nanofibers

Biocompatibility is among essential features of designed and synthesized scaffolds for tissue engineering studies. Besides their bioactive epitopes, constituents of peptide nanofibers are natural components of cells, as alkyl tails are composed of carbon atoms and small amino acid chains are naturally found in the ECM environment. All glycopeptide scaffolds including sulfonate-including ones provide a proper environment for the viability of HUVECs and PC-12 cells (Figure 17, 18, 19).

Galactose/K-PA   Mannose/K-PA   Glucose/K-PA

N-Acetylglucosamine/K-PA   EE/K-PA

Galactose/SO$_3$/K-PA   Mannose/SO$_3$/K-PA   Glucose/SO$_3$/K-PA

N-Acetylglucosamine/SO$_3$/K-PA   SO$_3$/K-PA
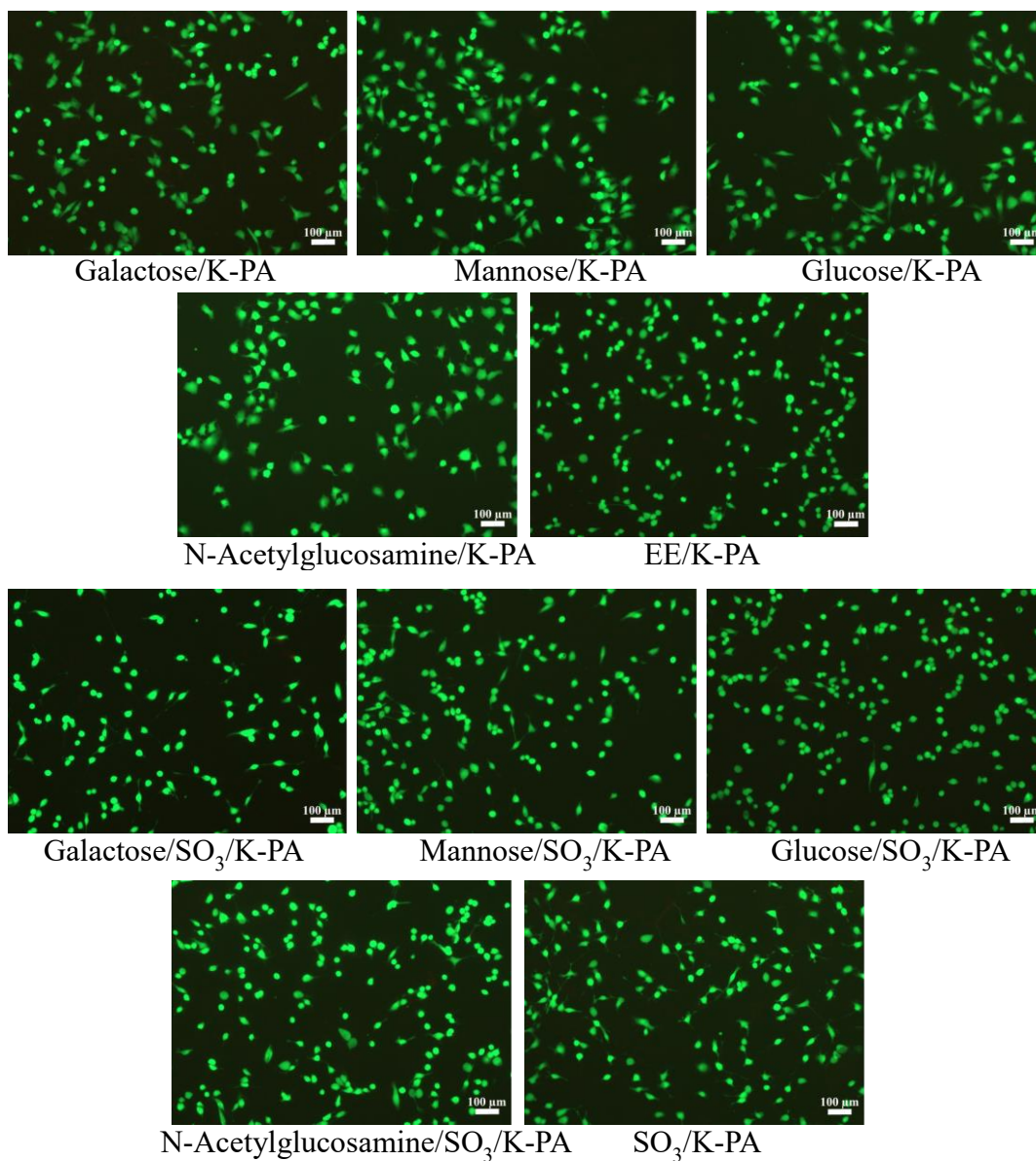
Figure 17: Representative images of live-dead assay of HUVECs that are cultured on glycopeptide nanofibers. Green dots indicate live cells (calcein-AM) and red dots indicate dead cells (ethidium homodimer).
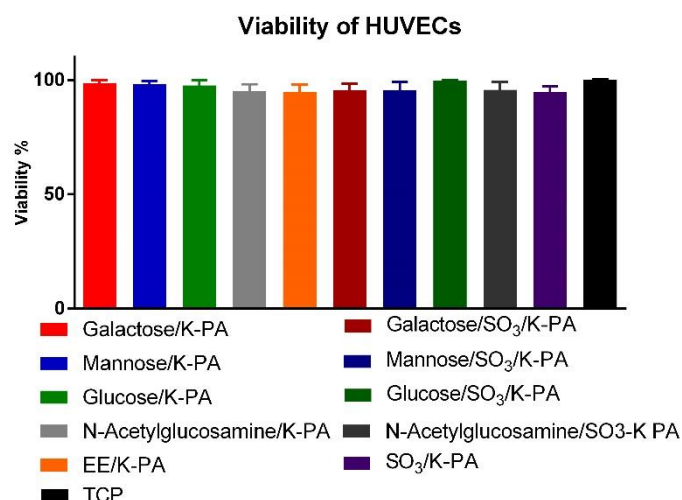
Figure 18: Results of live-dead assay indicate that all glycopeptide nanofibers are biocompatible.
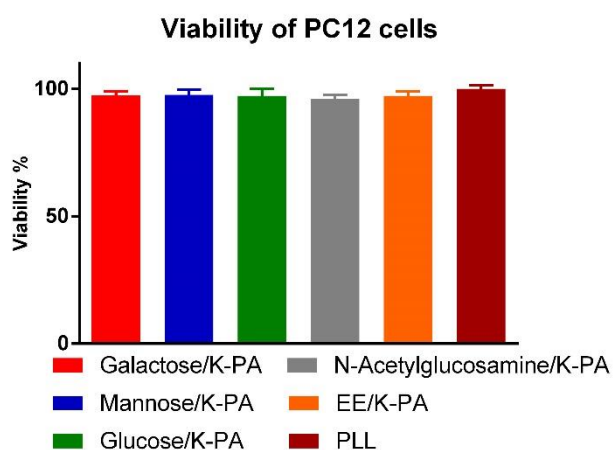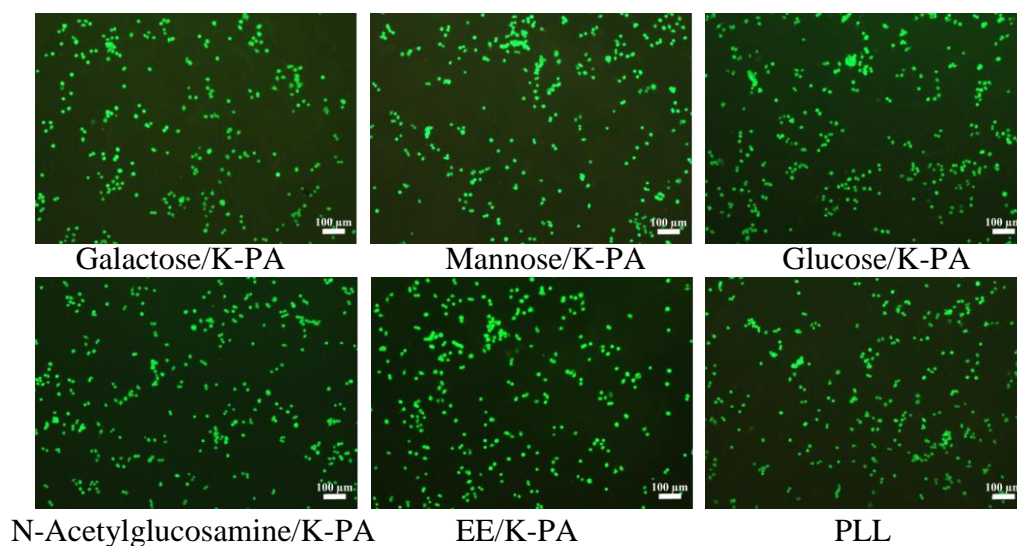
Figure 19: Representative images of PC-12 cells and quantification of live dead assay.

2.3.4. Glycopeptide-Sulfonate Nanofiber Networks Promote *in vitro* Tube-like Structures

Angiogenesis induction potential of glycopeptide nanofibers and glycopeptide-sulfonate nanofibers was further investigated via *in vitro* tube formation assay. HUVECs have the ability to form tube-like structures when they are stimulated with pro-angiogenic factors such as VEGF and FGF-2 [84]. As previously stated, GAGs consist of repeated disaccharide units modified with sulfonated or N-acetylated sugars. The glycopeptide nanofibers had less affinity to VEGF and FGF-2 than SO_3-PA-added ones (Figure 15) and they did not form any tube-like structures (Figure 20 a). Although SO_3-PA has a significantly higher affinity for VEGF and FGF-2, SO_3 presence alone was not sufficient for tube formation. However, the combinations of glycopeptide-PAs and SO_3-PA were able to induce the formation of tube-like structures without additional pro-angiogenic factors (Figure 20 b). Despite N-acetylated amino sugars and the oxidated form of glucose (a hydroxyl group that is converted into a carboxyl group) that are present in the structures of GAGs, galactose/SO_3-PA and mannose/SO_3-PA nanofibers demonstrated significantly higher tube length induction and form ordered tube-like structures to a greater extent than glucose/ SO_3-PA and N-acetylglucosamine/ SO_3-PA nanofibers. The presence of carboxyl groups in the structure of nanofiber networks is crucial for tube formation, as very few tube-like structures were observed in HUVECs cultured on EE/K-PA nanofibers, despite the higher affinity of this combination to VEGF and FGF-2. Therefore, we conclude that the existence of sulfate and carboxyl groups together with sugar units is indispensable for the coordinated formation of tubular structures *in vitro*.

a)

Galactose/K-PA   Mannose/K-PA   Glucose/K-PA

N-Acetylglucosamine/K-PA   SO₂/K-PA

b)

Galactose/SO$_3$/K-PA   Mannose/SO$_3$/K-PA   Glucose/SO$_3$/K-PA

N-Acetylglucosamine/SO$_3$/K-PA   EE/K-PA

c)

Figure 20: Brightfield microscope images of HUVECs cultured on nanofibers. Tube formation assay quantification, average length of formed tubular structures. Values represent mean ±SEM (***p<0.001).

2.3.5. Glycopeptide Nanofibers Enhance Neurite Extension

Patterns of the NGF affinity of glycopeptides led us to investigate their effects on PC-12 cells, which are neuron-like and NGF-responsive. Previously, heparin-conjugated fibrin matrices were used to control the slow and sustained release of NGF. In these studies, heparin was assumed to immobilize NGF while fibrin matrices provided a porous, ECM-mimetic network for the encapsulation of NGF [42, 85]. In here, we demonstrated that glucose and N-acetylglucosamine bearing nanofibers significantly enhanced and supported neurite outgrowth without NGF encapsulation inside these nanofiber systems (Figure 20). The NGF-binding potential of glycopeptides could be used to support nerve regeneration and the additional encapsulation of NGF to these nanofibers could create a favorable environment for the sustained and slow release of NGF.
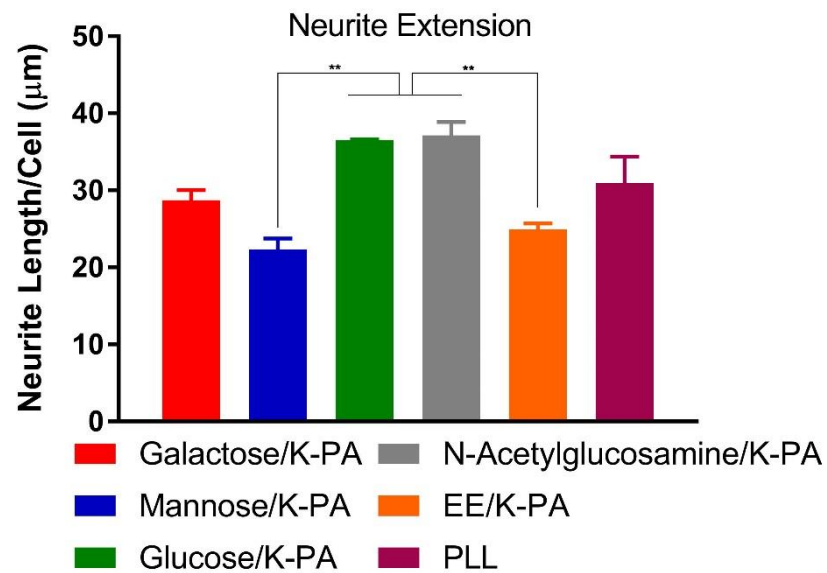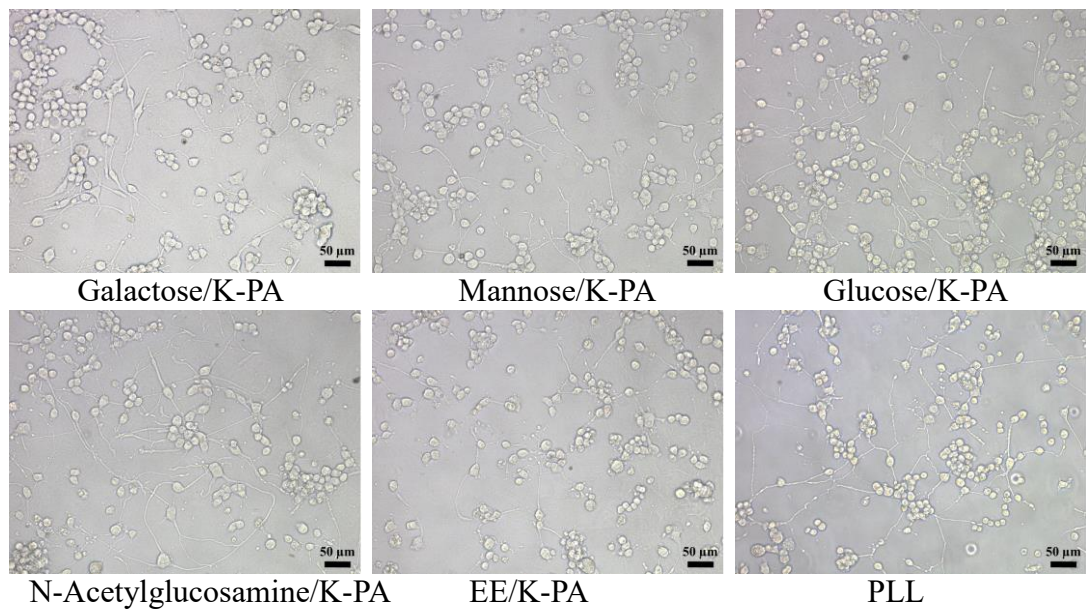
Figure 21: Brightfield microscope images of PC-12 cells cultured on glycopeptide nanofibers and quantification of average neurite extension. Values represent mean ±SEM (**p<0.01).

2.3.6. Time-Dependent VEGF and FGF-2 Secretion Analyses of HUVECs Cultured on Glycopeptide-Sulfonate Nanofibers

Glycopeptide-sulfonate nanofibers promoted tube-like structures without any exogenous angiogenic factor addition to the environment. Therefore, we sought to determine whether the glycopeptide-sulfonate nanofibers were able to store endogenously secreted VEGF and present this growth factor to cells in a convenient manner. Time-dependent VEGF secretion from HUVECs was analyzed using an ELISA based method. Secreted VEGF concentration gradually increased in all glycopeptide-sulfonate groups until 36 h (Figure 23). This release pattern could be related to the autocrine signaling of VEGF, as tube-like structures were observed at the end of 36 hours. Galactose-sulfonate and mannose-sulfonate nanofibers, which formed more ordered tube-like structures and had higher average tube lengths at the end of 36 h, secreted the highest concentration of VEGF even compared to other glycopeptide-sulfonate nanofibers. At 48 h, VEGF concentration of galactose-sulfonate and mannose-sulfonate nanofibers decreased and came to a similar level with glucose-sulfonate and N-acetylglucosamine-sulfonate nanofibers. However, sulfonate and EE/K-PA control nanofibers exhibited a lower level of VEGF secretion throughout 48 h compared to glycopeptide-sulfonate nanofibers. Low levels of VEGF secretion could be due to a strong affinity between secreted VEGF from HUVECs and sulfonate and EE/K-PA nanofibers, and this concentrated binding may have inhibited the autocrine signaling of VEGF and induced the formation of few to no tube-like structures. Additionally, despite the presence of carboxyl and sulfonate groups, this combination does not resemble GAGs as much as the glycopeptide-sulfonate

nanofibers. Thus galactose-sulfonate and mannose-sulfonate nanofibers created much more GAG-mimetic nanostructures and efficiently enhanced *in vitro* tube formation. We also analyzed the FGF-2 release profiles of HUVECs cultured on glycopeptide-sulfonate nanofibers (Figure 22). At each time point, there were no significant differences between all groups except FGF-2 release from HUVECs cultured on mannose-sulfonate nanofibers. These results suggest that VEGF binding to and release from glycopeptide-sulfonate nanofibers is the principal factor for directing tube formation.
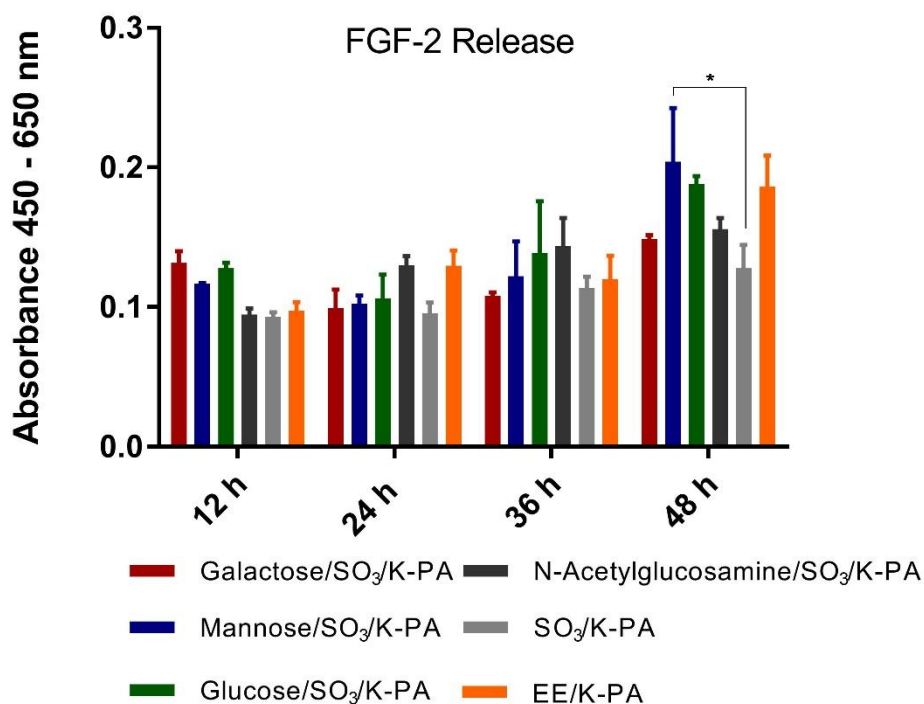
Figure 22: FGF-2 release profiles of HUVECs cultured on glycopeptide-sulfonate nanofibers.
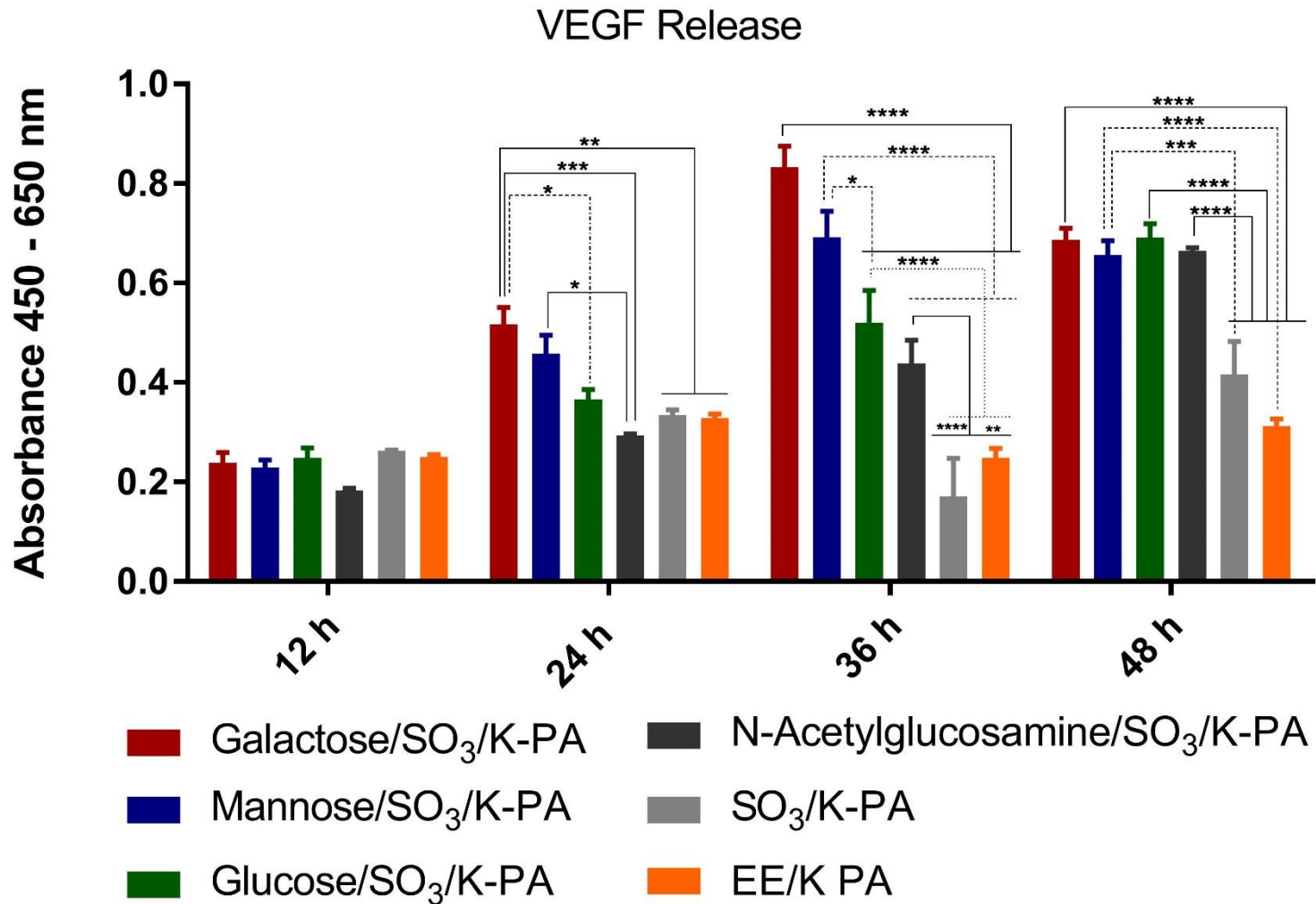
Figure 23: Time dependent release of VEGF secreted from HUVECs cultured on glycopeptide-sulfonate nanofibers.

Values represent mean ±SEM (****p<0.0001).

2.4. Conclusions and Future Perspectives

Growth factors participate in many crucial events, including the development of organisms, morphogenesis and tissue regeneration. Growth factor-based tissue engineering strategies gave promising outcomes and some are now commercially available for therapeutic purposes [86, 87]. However, shortcomings of delivery systems require the development of new techniques to further optimize the tissue recovery process. Therefore, manipulating and controlling the presentation, degradation rate, release rate and retention time of growth factors at the targeted site is a promising approach for directing the fate of cells or tissues in tissue regeneration studies. To date, a variety of methods have been designed and investigated for this purpose. Naturally derived scaffolds (polymers and polysaccharides), for example, are commonly used for tissue regeneration studies. However, despite advantages such as high biocompatibility, the native presence of cell adhesive structures and ease of adaptation to biological environments; issues such as batch-to-batch variations and immunogenicity are limiting factors for the use of naturally derived materials in tissue regeneration [88]. Synthetic biomaterials such as polymers and self-assembled systems are produced to overcome these disadvantages, and polymeric hydrogels are generally preferred due to their high-hydration capacity and ECM-mimetic porous network structures [39]. Additionally, hybrid scaffolds have been produced by combining synthetic polymers and natural ECM elements and used to deliver growth factors through their immobilization within biological components and controlled release through the synthetic material [89]. Since GAGs are one of the essential modulators of growth factor behaviors in ECM, GAG-based delivery strategies are highly promising. Both the incorporation of GAGs in scaffolds and the design and

47

synthesis of GAG-mimetic self-assembled scaffolds are promising approaches for growth factor presentation. Here, we imitated the GAG units of the ECM using sugar-containing self-assembled PA molecules. While their β-sheet forming unit enables the formation of ECM-like porous structures, their modifiable end-site provides a design opportunity to add bioactive epitopes to the network. In our case, PA molecules were functionalized with galactose, mannose, glucose and N-acetylglucosamine sugars and mixed with oppositely-charged, lysine-containing PAs to form nanofibrous structures. In addition, a SO_3-bearing PA was added to the system to obtain a structure more similar to GAGs. All PA combinations were physicochemically characterized, and all were found to exhibit a β-sheet signal on CD spectroscopy analyses (Figure 11). Nanofibrous structures of scaffolds were further characterized by AFM which showed their morphology (Figure 13). These nanofiber systems were further analyzed on the basis of their interactions with growth factors and ability to present them to cells. The affinity of glycopeptides against VEGF and FGF-2 molecules was investigated. While glycopeptide nanofibers showed low affinity against VEGF and FGF-2, their SO_3-added combinations demonstrated high binding (Figure 14). Since VEGF and FGF-2 have heparin-binding domains, the heparin-mimetic conformation of molecules is expected to show higher affinity. Among their SO_3-added combinations, N-acetylglucosamine- SO_3 nanofiber showed the lowest affinity to VEGF and FGF-2. Although one of the disaccharide units of heparin consists of N-acetylglucosamine, without N-sulfation the sugar moiety alone may not be sufficient to strongly bind to VEGF. In addition, only SO_3-PA and EE/K-PA gave high absorbance in VEGF and FGF-2 binding analyses. The possible reason for this effect may be the ability of these combinations to better display SO_3 and carboxyl groups on their surface. It is known

that 2-O, 6-O and N-sulfation and carboxyl groups are crucial determinants of the VEGF-heparin interaction [83].

Additionally, glycopeptide nanofibers were tested for NGF-binding capacity. In contrast to VEGF and FGF-2, NGF showed a strong affinity towards glycopeptide nanofibers. Heparin-based scaffolds have previously been used in NGF delivery for peripheral nerve regeneration [42, 85]. However, as NGF does not contain a heparin-binding domain, we analyzed only glycopeptide nanofibers and observed a high capacity for NGF binding (Figure 15).

Effects of glycopeptide nanofibers and glycopeptide- SO_3 nanofibers on endothelial and NGF responsive PC-12 cells were also investigated. Since biocompatibility is one of the most important features of scaffolds, the viability of cells was analyzed by culturing them on glycopeptide nanofibers. Live-dead assay analyses revealed that the nanofibers formed a habitable and friendly environment for HUVECs and PC-12 cells (Figure 17, 18, 19). Considering that VEGF and FGF-2 are pro-angiogenic growth factors, their affinity to glycopeptide- SO_3 nanofibers may promote angiogenesis. Thus, we tested the *in vitro* tube formation capacity of glycopeptide nanofibers. Sugar-containing nanofibers alone did not induce the formation of any capillary structures (Figure 19 a). However, their SO_3-PA added combinations promoted tube-like structures without any exogenous VEGF or FGF-2 addition (Figure 19 b). Quantification of tube lengths revealed that galactose- SO_3 and mannose-SO_3 nanofibers formed much more ordered tubes and had significantly higher tube lengths compared to glucose- SO_3 and N-acetylglucosamine- SO_3 nanofibers. SO_3, carboxyl and hydroxyl groups may be presented on the surface of these nanofibers to a greater extent due to a relative lack of steric hindrance. EE/K-PA nanofibers also induced the

formation of few tube like structures. The reason for that may be the presence of several hydroxyl groups on the structure of EE-PA. Effects of glycopeptide nanofibers on NGF responsive PC-12 cells were also evaluated due to their high affinity to NGF. All glycopeptides induced extension of the neurites of PC-12 cells, and N-acetylglucosamine and glucose nanofibers demonstrated significantly higher neurite lengths. Considering their affinity to NGF and high neurite extension capacity, these groups could be used as NGF encapsulation agents and implanted to regenerate peripheral nerve injuries due to their capacity to release NGF sustainably. They can also create a biocompatible and ECM-like environment to support the migration and differentiation of cells in these injuries.

Since tube-like structures were formed without exogenous angiogenic stimulants, release profiles of VEGF and FGF-2 were analyzed to determine whether the PA systems are capable of controlled release. All glycopeptide- SO_3 combinations released VEGF increasingly throughout 48 h. However, galactose- SO_3 and mannose-SO_3 nanofibers exhibited a peak at 36 h, which was parallel with tube length quantification. VEGF secretion from another glycopeptide- SO_3 nanofibers reached the same level with galactose- SO_3 and mannose- SO_3 nanofibers at 48 h, but VEGF released from these groups was nevertheless lower than the record set by galactose- SO_3 and mannose- SO_3 groups at 36 h. This release pattern may be an indicator of autocrine signaling by VEGF, and it is plausible that these nanofibers store endogenously secreted VEGF to present it to the cells in a more accessible configuration. In addition, the secretion of VEGF from HUVECs was limited on SO_3 and EE/K-PA nanofibers, which showed high absorbance profiles in ELISA-based affinity analyses. Few tube-like structures were present on EE/K-PA and these structures were altogether absent

on SO3/K-PA nanofibers, possibly due to the strong affinity of VEGF to these scaffolds preventing its release. Thus, the existence of glyco-PA and SO_3 groups on nanofibers is required for *in vitro* tube formation, but the excess of a single group may be detrimental. In addition, FGF-2 release from HUVECs was analyzed and revealed no significant differences in between the groups at each time point. Therefore, VEGF appears to be the main modulator of tube-like structure formation.

All in all, in this thesis we demonstrate that GAG-mimetic, sugar-containing and SO_3-functionalized combinations of peptide nanofibers can promote *in vitro* tube formation by exhibiting an adequate affinity to VEGF. In addition, the generated glycopeptide nanofibers are strongly affine to NGF and support the neurite extension of PC-12 cells. Following further characterization of the tube formation and neurite extension mechanisms, these nanofibers can be used in *in vivo* applications to present growth factors for regeneration. Additionally, combinations of multiple growth factors can be delivered to the target area depending on the needs of individual tissues and injuries; *e.g.* in cases where both angiogenesis and nerve regeneration are desired.

GAGs surround all types of cells and actively participate in signal transduction pathways to determine the behavior of cells. Therefore, GAG-mimicking scaffolds are promising candidates for the regeneration of a variety of tissues. Supplementation of oxygen and nutrients is a necessary step of regeneration. Creation of angiogenesis-supportive scaffolds will have a broad range of usage in supporting many aspects of regeneration, considering the key roles of blood vessel formation for the regeneration of injured tissues. Here, a designed glycopeptide PA array created structures that strongly resemble natural GAG networks thanks to their monosaccharide units. Together with SO_3 addition, they were bioactively functional and directed the cells

towards behaviors consistent with their growth factor interactions. These PA platforms could be used efficiently to deliver growth factors in precise concentrations, which is crucial to support cellular growth without hypertrophy. Due to their affinity to growth factors, their encapsulation and release processes could be easily adapted for clinical purposes to provide enhanced and shortened healing under *in vivo* conditions.

Glycobiology is a challenging research subject due to the difficulty inherent to the isolation of each individual unit and identification of their functions outside the context of other glycoconjugates, which typically cannot be separated because of their structural multiplicity and heterogeneity in cells. Therefore, monosaccharide-bearing PA arrays could be utilized to reveal the functions of each monosaccharide independently for specific cellular events, which is accomplished in a facile manner due to the relative ease of preparation and manipulation of glycosylated PAs. Specifically, proteins-sugar interactions could be identified and further characterized with the aid of the glycopeptide array described in the present study.

Bibliography

1. Freudenberg, U., et al., *Glycosaminoglycan-Based Biohybrid Hydrogels: A Sweet and Smart Choice for Multifunctional Biomaterials.* Advanced Materials, 2016. **28**(40): p. 8861-8891.

2. Aamodt, J.M. and D.W. Grainger, *Extracellular matrix-based biomaterial scaffolds and the host response.* Biomaterials, 2016. **86**: p. 68-82.

3. Karsdal, M.A., et al., *Novel insights into the function and dynamics of extracellular matrix in liver fibrosis.* American Journal of Physiology Gastrointestinal Liver Physiology, 2015. **308**(10): p. G807-30.

4. Frantz, C., K.M. Stewart, and V.M. Weaver, *The extracellular matrix at a glance.* Journal of Cell Science, 2010. **123**(Pt 24): p. 4195-200.

5. Theocharis, A.D., et al., *Extracellular matrix structure.* Advanced Drug Delivery Reviews, 2016. **97**: p. 4-27.

6. Bosman, F.T. and I. Stamenkovic, *Functional structure and composition of the extracellular matrix.* The Journal of Pathology, 2003. **200**(4): p. 423-8.

7. Shoulders, M.D. and R.T. Raines, *Collagen structure and stability.* Annual Review of Biochemistry, 2009. **78**: p. 929-58.

8. Gordon, M.K. and R.A. Hahn, *Collagens.* Cell and Tissue Research, 2010. **339**(1): p. 247-57.

9. Kielty, C.M., *Elastic fibres in health and disease.* Expert Reviews in Molecular Medicine, 2006. **8**(19): p. 1-23.

10. Alberts, B., et al., *The Extracellular Matrix of Animals*. 4th edition 2002, New York: Garland Science.

11. George, E.L., et al., *Defects in mesoderm, neural tube and vascular development in mouse embryos lacking fibronectin.* Development, 1993. **119**(4): p. 1079-91.

12. Pankov, R. and K.M. Yamada, *Fibronectin at a glance.* Journal of Cell Science, 2002. **115**(Pt 20): p. 3861-3.

13. Rovensky, Y.A., *The Extracellular Matrix*. 2011, Adhesive Interactions in Normal and Transformed Cells.

14. Halfter, W., et al., *New concepts in basement membrane biology.* The FEBS Journal, 2015. **282**(23): p. 4466-79.

15. Iozzo, R.V. and L. Schaefer, *Proteoglycan form and function: A comprehensive nomenclature of proteoglycans.* Matrix Biology, 2015. **42**: p. 11-55.

16. Lawrence, R., et al., *Disaccharide structure code for the easy representation of constituent oligosaccharides from glycosaminoglycans.* Nature Methods, 2008. **5**(4): p. 291-2.

17. Sasisekharan, R. and G. Venkataraman, *Heparin and heparan sulfate: biosynthesis, structure and function.* Current Opinion in Chemical Biology, 2000. **4**(6): p. 626-31.

18. Itano, N., *Simple primary structure, complex turnover regulation and multiple roles of hyaluronan.* The Journal of Biochemistry, 2008. **144**(2): p. 131-7.

19. Lauder, R.M., *Chondroitin sulphate: a complex molecule with potential impacts on a wide range of biological systems.* Complementary Therapies in Medicine, 2009. **17**(1): p. 56-62.

20. Thelin, M.A., et al., *Biological functions of iduronic acid in chondroitin/dermatan sulfate.* The FEBS Journal, 2013. **280**(10): p. 2431-46.

21. Funderburgh, J.L., *Keratan sulfate: structure, biosynthesis, and function.* Glycobiology, 2000. **10**(10): p. 951-8.

22.   Wardrop, D. and D. Keeling, *The story of the discovery of heparin and warfarin.* British Journal of Haematology, 2008. **141**(6): p. 757-63.

23.   Bishop, J.R., M. Schuksz, and J.D. Esko, *Heparan sulphate proteoglycans fine-tune mammalian physiology.* Nature, 2007. **446**(7139): p. 1030-7.

24.   Babensee, J.E., L.V. McIntire, and A.G. Mikos, *Growth factor delivery for tissue engineering.* Pharmaceutical Research, 2000. **17**(5): p. 497-504.

25.   Rouwkema, J., N.C. Rivron, and C.A. van Blitterswijk, *Vascularization in tissue engineering.* Trends in Biotechnology, 2008. **26**(8): p. 434-41.

26.   Hoeben, A., et al., *Vascular endothelial growth factor and angiogenesis.* Pharmacological Reviews, 2004. **56**(4): p. 549-80.

27.   Robinson, C.J., et al., *VEGF165-binding sites within heparan sulfate encompass two highly sulfated domains and can be liberated by K5 lyase.* The Journal of Biological Chemistry, 2006. **281**(3): p. 1731-40.

28.   Armelin, H.A., *Pituitary extracts and steroid hormones in the control of 3T3 cell growth.* Proceedings of the National Academy of Sciences of the United States of America, 1973. **70**(9): p. 2702-6.

29.   Beenken, A. and M. Mohammadi, *The FGF family: biology, pathophysiology and therapy.* Nature Reviews Drug Discovery, 2009. **8**(3): p. 235-53.

30.   Nickel, W., *Unconventional secretion: an extracellular trap for export of fibroblast growth factor 2.* Journal of Cell Science, 2007. **120**(Pt 14): p. 2295-9.

31.   Harmer, N.J., *Insights into the role of heparan sulphate in fibroblast growth factor signalling.* Biochemical Society Transactions, 2006. **34**(Pt 3): p. 442-5.

32.   Kreuger, J., et al., *Interactions between heparan sulfate and proteins: the concept of specificity.* The Journal of Cell Biology, 2006. **174**(3): p. 323-7.

33.   Yarski, M.A., et al., *Nerve growth factor alpha subunit: effect of site-directed mutations on catalytic activity and 7S NGF complex formation.* Biochimica Biophysica Acta, 2000. **1477**(1-2): p. 253-66.

34.   Chao, M.V. and B.L. Hempstead, *p75 and Trk: a two-receptor system.* Trends in Neurosciences, 1995. **18**(7): p. 321-6.

35.   Rogers, C.J., et al., *Elucidating glycosaminoglycan-protein-protein interactions using carbohydrate microarray and computational approaches.* Proceedings of the National Academy of Sciences of the United States of America, 2011. **108**(24): p. 9747-52.

36.   Miller, G.M. and L.C. Hsieh-Wilson, *Sugar-dependent modulation of neuronal development, regeneration, and plasticity by chondroitin sulfate proteoglycans.* Experimental Neurology, 2015. **274**(Pt B): p. 115-25.

37.   Simons, M., et al., *Pharmacological treatment of coronary artery disease with recombinant fibroblast growth factor-2: double-blind, randomized, controlled clinical trial.* Circulation, 2002. **105**(7): p. 788-93.

38.   Henry, T.D., et al., *The VIVA trial: Vascular endothelial growth factor in Ischemia for Vascular Angiogenesis.* Circulation, 2003. **107**(10): p. 1359-65.

39.   Tibbitt, M.W. and K.S. Anseth, *Hydrogels as extracellular matrix mimics for 3D cell culture.* Biotechnology and Bioengineering, 2009. **103**(4): p. 655-63.

40.   Sakiyama-Elbert, S.E., A. Panitch, and J.A. Hubbell, *Development of growth factor fusion proteins for cell-triggered drug delivery.* The FASEB Journal, 2001. **15**(7): p. 1300-2.

41.   Zisch, A.H., et al., *Covalently conjugated VEGF--fibrin matrices for endothelialization.* Journal of Controlled Release, 2001. **72**(1-3): p. 101-13.

42.   Sakiyama-Elbert, S.E. and J.A. Hubbell, *Controlled release of nerve growth factor from a heparin-containing fibrin-based cell ingrowth matrix.* Journal of Controlled Release, 2000. **69**(1): p. 149-58.

43.   Silva, E.A., et al., *Material-based deployment enhances efficacy of endothelial progenitor cells.* Proceedings of the National Academy of Sciences of the United States of America, 2008. **105**(38): p. 14347-52.

44.   Rocha, F.G., et al., *The effect of sustained delivery of vascular endothelial growth factor on angiogenesis in tissue-engineered intestine.* Biomaterials, 2008. **29**(19): p. 2884-90.

45.   Benoit, D.S. and K.S. Anseth, *Heparin functionalized PEG gels that modulate protein adsorption for hMSC adhesion and differentiation.* Acta Biomaterialia, 2005. **1**(4): p. 461-70.

46.   Benoit, D.S., A.R. Durney, and K.S. Anseth, *The effect of heparin-functionalized PEG hydrogels on three-dimensional human mesenchymal stem cell osteogenic differentiation.* Biomaterials, 2007. **28**(1): p. 66-77.

47.   Cai, S., et al., *Injectable glycosaminoglycan hydrogels for controlled release of human basic fibroblast growth factor.* Biomaterials, 2005. **26**(30): p. 6054-67.

48.   Tanihara, M., et al., *Sustained release of basic fibroblast growth factor and angiogenesis in a novel covalently crosslinked gel of heparin and alginate.* Journal of Biomedical Materials Research, 2001. **56**(2): p. 216-21.

49.   Boekhoven, J. and S.I. Stupp, *25th anniversary article: supramolecular materials for regenerative medicine.* Advanced Materials, 2014. **26**(11): p. 1642-59.

50.   Webber, M.J., et al., *Supramolecular biomaterials.* Nature Materials, 2016. **15**(1): p. 13-26.

51. Tsurkan, M.V., et al., *Defined polymer-peptide conjugates to form cell-instructive starPEG-heparin matrices in situ.* Advanced Materials, 2013. **25**(18): p. 2606-10.

52. Rajangam, K., et al., *Heparin binding nanostructures to promote growth of blood vessels.* Nano Letters, 2006. **6**(9): p. 2086-90.

53. Webber, M.J., et al., *Capturing the stem cell paracrine effect using heparin-presenting nanofibres to treat cardiovascular diseases.* Journal of Tissue Engineering and Regenerative Medicine, 2010. **4**(8): p. 600-10.

54. Lee, S.S., et al., *Gel scaffolds of BMP-2-binding peptide amphiphile nanofibers for spinal arthrodesis.* Advanced Healthcare Materials, 2015. **4**(1): p. 131-141.

55. Mammadov, R., et al., *Heparin mimetic peptide nanofibers promote angiogenesis.* Biomacromolecules, 2011. **12**(10): p. 3508-19.

56. Mammadov, R., et al., *Growth factor binding on heparin mimetic peptide nanofibers.* Biomacromolecules, 2012. **13**(10): p. 3311-9.

57. Uzunalli, G., et al., *Angiogenic Heparin-Mimetic Peptide Nanofiber Gel Improves Regenerative Healing of Acute Wounds*. 2016, American Chemical Society: ACS Biomaterials Science & Engineering. p. 1296–1303.

58. Yergoz, F., et al., *Heparin mimetic peptide nanofiber gel promotes regeneration of full thickness burn injury.* Biomaterials, 2017. **134**: p. 117-127.

59. Uzunalli, G., et al., *Improving pancreatic islet in vitro functionality and transplantation efficiency by using heparin mimetic peptide nanofiber gels.* Acta Biomaterialia, 2015. **22**: p. 8-18.

60. Rufaihah, A.J., et al., *Angiogenic peptide nanofibers repair cardiac tissue defect after myocardial infarction.* Acta Biomaterialia, 2017. **58**: p. 102-112.

61. Ustun, S., et al., *Growth and differentiation of prechondrogenic cells on bioactive self-assembled peptide nanofibers.* Biomacromolecules, 2013. **14**(1): p. 17-26.

62. Kocabey, S., et al., *Glycosaminoglycan mimetic peptide nanofibers promote mineralization by osteogenic cells.* Acta Biomaterialia, 2013. **9**(11): p. 9075-85.

63. Tansik, G., et al., *A glycosaminoglycan mimetic peptide nanofiber gel as an osteoinductive scaffold.* Biomaterials Science, 2016. **4**(9): p. 1328-39.

64. Tabata, Y., *Tissue regeneration based on growth factor release.* Tissue Engineering, 2003. **9 Suppl 1**: p. S5-15.

65. Martino, M.M., et al., *Engineering the growth factor microenvironment with fibronectin domains to promote wound and bone tissue healing.* Science Translational Medicine, 2011. **3**(100): p. 100ra89.

66. Lutolf, M.P., et al., *Repair of bone defects using synthetic mimetics of collagenous extracellular matrices.* Nature Biotechnology, 2003. **21**(5): p. 513-8.

67. Holland, T.A. and A.G. Mikos, *Advances in drug delivery for articular cartilage.* Journal of Controlled Release, 2003. **86**(1): p. 1-14.

68. Yang, W., et al., *Chondrogenic differentiation on perlecan domain I, collagen II, and bone morphogenetic protein-2-based matrices.* Tissue Engineering, 2006. **12**(7): p. 2009-24.

69. Backer, M.V., et al., *Surface immobilization of active vascular endothelial growth factor via a cysteine-containing tag.* Biomaterials, 2006. **27**(31): p. 5452-8.

70. Zisch, A.H., et al., *Cell-demanded release of VEGF from synthetic, biointeractive cell ingrowth matrices for vascularized tissue growth.* The FASEB Journal, 2003. **17**(15): p. 2260-2.

71. Hudalla, G.A. and W.L. Murphy, *Biomaterials that regulate growth factor activity via bioinspired interactions.* Advanced Functional Materials, 2011. **21**(10): p. 1754-1768.

72.   Martino, M.M., et al., *Extracellular matrix and growth factor engineering for controlled angiogenesis in regenerative medicine.* Frontiers in Bioengineering and Biotechnology, 2015. **3**: p. 45.

73.   Shute, J., *Glycosaminoglycan and chemokine/growth factor interactions.* Handbook of Experimental Pharmacology, 2012(207): p. 307-24.

74.   Lee, K., E.A. Silva, and D.J. Mooney, *Growth factor delivery-based tissue engineering: general approaches and a review of recent developments.* Journal of The Royal Society Interface, 2011. **8**(55): p. 153-70.

75.   Nillesen, S.T., et al., *Increased angiogenesis and blood vessel maturation in acellular collagen-heparin scaffolds containing both FGF2 and VEGF.* Biomaterials, 2007. **28**(6): p. 1123-31.

76.   Liu, Y., et al., *Release of basic fibroblast growth factor from a crosslinked glycosaminoglycan hydrogel promotes wound healing.* Wound Repair and Regeneration, 2007. **15**(2): p. 245-51.

77.   Sakiyama-Elbert, S.E. and J.A. Hubbell, *Development of fibrin derivatives for controlled release of heparin-binding growth factors.* Journal of Controlled Release, 2000. **65**(3): p. 389-402.

78.   Ehrbar, M., et al., *The role of actively released fibrin-conjugated VEGF for VEGF receptor 2 gene activation and the enhancement of angiogenesis.* Biomaterials, 2008. **29**(11): p. 1720-9.

79.   Traub, S., et al., *The promotion of endothelial cell attachment and spreading using FNIII10 fused to VEGF-A165.* Biomaterials, 2013. **34**(24): p. 5958-68.

80.   Impellitteri, N.A., et al., *Specific VEGF sequestering and release using peptide-functionalized hydrogel microspheres.* Biomaterials, 2012. **33**(12): p. 3475-84.

81.   Arslan, E., M.O. Guler, and A.B. Tekinay, *Glycosaminoglycan-Mimetic Signals Direct the Osteo/Chondrogenic Differentiation of Mesenchymal Stem Cells in a Three-Dimensional Peptide Nanofiber Extracellular Matrix Mimetic Environment.* Biomacromolecules, 2016. **17**(4): p. 1280-91.

82.   Mammadov, B., et al., *Cooperative effect of heparan sulfate and laminin mimetic peptide nanofibers on the promotion of neurite outgrowth.* Acta Biomaterialia, 2012. **8**(6): p. 2077-86.

83.   Zhao, W., et al., *Binding affinities of vascular endothelial growth factor (VEGF) for heparin-derived oligosaccharides.* Bioscience Reports, 2012. **32**(1): p. 71-81.

84.   Staton, C.A., M.W. Reed, and N.J. Brown, *A critical analysis of current in vitro and in vivo angiogenesis assays.* International Journal of Experimental Pathology, 2009. **90**(3): p. 195-221.

85.   Lee, A.C., et al., *Controlled release of nerve growth factor enhances sciatic nerve regeneration.* Experimental Neurology, 2003. **184**(1): p. 295-303.

86.   Govender, S., et al., *Recombinant human bone morphogenetic protein-2 for treatment of open tibial fractures: a prospective, controlled, randomized study of four hundred and fifty patients.* The Journal of Bone and Joint Surgery American volume, 2002. **84-A**(12): p. 2123-34.

87.   Vaccaro, A.R., et al., *The safety and efficacy of OP-1 (rhBMP-7) as a replacement for iliac crest autograft for posterolateral lumbar arthrodesis: minimum 4-year follow-up of a pilot study.* The Spine Journal, 2008. **8**(3): p. 457-65.

88.   Malafaya, P.B., G.A. Silva, and R.L. Reis, *Natural-origin polymers as carriers and scaffolds for biomolecules and cell delivery in tissue engineering applications.* Advanced Drug Delivery Reviews, 2007. **59**(4-5): p. 207-33.

89.   Silva, A.K., et al., *Growth factor delivery approaches in hydrogels.* Biomacromolecules, 2009. **10**(1): p. 9-18.